



**HAL**  
open science

## Calcium isotopes in enamel of modern and Plio-Pleistocene East African mammals

J.E. E Martin, T. Tacail, T. E. Cerling, V. Balter

### ► To cite this version:

J.E. E Martin, T. Tacail, T. E. Cerling, V. Balter. Calcium isotopes in enamel of modern and Plio-Pleistocene East African mammals. *Earth and Planetary Science Letters*, 2018, 503, pp.227-235. 10.1016/j.epsl.2018.09.026 . hal-02568580

**HAL Id: hal-02568580**

**<https://hal.science/hal-02568580v1>**

Submitted on 9 May 2020

**HAL** is a multi-disciplinary open access archive for the deposit and dissemination of scientific research documents, whether they are published or not. The documents may come from teaching and research institutions in France or abroad, or from public or private research centers.

L'archive ouverte pluridisciplinaire **HAL**, est destinée au dépôt et à la diffusion de documents scientifiques de niveau recherche, publiés ou non, émanant des établissements d'enseignement et de recherche français ou étrangers, des laboratoires publics ou privés.

1 **Calcium isotopes in enamel of modern and Plio-Pleistocene East African**  
2 **mammals**

3 J.E.Martin<sup>a</sup>, T.Tacail<sup>a</sup>, T.E.Cerling<sup>b</sup>, V.Balter<sup>a</sup>

4

5 <sup>a</sup>Laboratoire de Géologie de Lyon: Terre, Planète, Environnement, UMR CNRS 5276  
6 (CNRS, ENS, Université Lyon1), Ecole Normale Supérieure de Lyon, 69364 Lyon  
7 cedex 07, France

8

9 <sup>b</sup>Department of Geology and Geophysics & Department of Biology, University of  
10 Utah, Salt Lake City, Utah 84112, USA

11

12 **Abstract**

13 Calcium isotope analyses show a depletion of heavy calcium isotopes in vertebrates,  
14 compared to food sources along each trophic step. Recent studies show considerable  
15 variability of the calcium isotopic composition of bone and teeth in modern mammals,  
16 leading to inconclusive interpretations regarding the utility of Ca isotopes for trophic  
17 inference in mammal-dominated terrestrial ecosystems. Here, we analyzed modern  
18 enamel samples from the Tsavo National Park (Kenya), and fossil enamel samples  
19 dated from *ca.* 4 Ma to 1.6 Ma from the Turkana Basin (Kenya). We found a  
20 constancy of taxa ordering between the modern and fossil datasets, suggesting that the  
21 diagenesis of calcium isotopes is minimal in fossils. In modern herbivore samples  
22 using similar digestive physiologies, browsers are enriched in <sup>44</sup>Ca compared to  
23 grazers. Both grazer and browser herbivore tooth enamel is enriched in <sup>44</sup>Ca relative  
24 to carnivores by about +0.30‰. Used together, carbon and calcium isotope  
25 compositions may help refine the structure of the C<sub>3</sub> and C<sub>4</sub> trophic chains in the fossil

26 record. Due to their high preservation potential, combining both carbon and calcium  
27 isotope systems represent a reliable approach to the reconstruction of the structure of  
28 past ecosystems.

29

## 30 **1. Introduction**

31 Calcium (Ca) is a major element (~40% weight) in carbonate hydroxylapatite  
32 (CHA): the inorganic phase of vertebrate phosphatic tissues (i.e., bone, enamel and  
33 dentine). Ca isotope ratios,  $^{44}\text{Ca}/^{40}\text{Ca}$  (here expressed as  $\delta^{44/42}\text{Ca}$ , see details  
34 thereafter), in vertebrate phosphatic tissues were first measured by means of thermal  
35 ionization mass spectrometry (Russell et al., 1978; Skulan et al., 1997; Skulan et al.,  
36 1999; Clementz et al., 2003). Ca stable isotope ratios have not been measured  
37 routinely by means of multi collector inductively coupled plasma mass spectrometry  
38 (MC-ICPMS) due to a major isobaric interference on  $^{40}\text{Ca}^+$  by  $^{40}\text{Ar}^+$ , and polyatomic  
39 and doubly charged interferences on  $^{42}\text{Ca}^+$ ,  $^{43}\text{Ca}^+$  and  $^{44}\text{Ca}^+$  beams (Wieser et al.,  
40 2004; Valdes et al., 2014; Tacail et al., 2016). Subsequent improvements of the Ca  
41 purification chemistry and in MC-ICPMS analytics further encouraged the interest of  
42 Ca isotope systematics in recent and fossil vertebrate samples with an emphasis at  
43 understanding mammal, fish and reptile biology and reconstruction of associated  
44 trophic chains (Clementz et al. 2003; Chu et al., 2006, Reynard et al., 2010, 2011,  
45 2013; Heuser et al., 2011; Melin et al., 2014; Martin et al., 2015, 2017a, 2017b; Tacail  
46 et al., 2017a; Hassler et al., 2018).

47 Two direct implications of the high Ca content in CHA stimulate the interest  
48 for the analysis of Ca isotopes. The first is that minute amount of phosphatic tissue,  
49 typically 100  $\mu\text{g}$ , is necessary to process the measurement of Ca isotope ratios  
50 accurately. Such a small amount of sample opens perspectives for the use of sample

51 leftovers or the almost non-destructive sampling of precious fossils. The second is that  
52 only extreme diagenesis, with more than 80% of reworked CHA, is predicted to have  
53 an effect on the original Ca isotope composition (Martin et al., 2017a). These  
54 calculations are made using water-rock interactions and assume that secondary  
55 calcium carbonates are leached accordingly. Collagen nitrogen is rarely preserved in  
56 fossils older than the Holocene or Late Pleistocene so that its potential as a trophic  
57 indicator in the deep past is precluded. Therefore, measuring Ca isotope ratios have  
58 the potential to allow reconstructing past trophic chains in vertebrate fossils of  
59 Pleistocene age and older. So far, only trace elements, mainly the strontium-calcium  
60 and barium-calcium ratios (Balter et al., 2001; Sponheimer and Lee-Thorp, 2006)  
61 have been used to this end, but trace elements have the disadvantage to be potentially  
62 altered by diagenetic processes (Reynard and Balter, 2014).

63       Trophic level reconstruction using Ca isotopes is based on the reasoning that  
64 the whole body tissues of vertebrates are depleted in heavy Ca isotopes relative to  
65 diet. The main observation is that bone Ca is depleted in heavy isotopes by -0.54‰ in  
66 average (expressed as  $\delta^{44/42}\text{Ca}$ ) when compared to dietary Ca in mammals (Skulan  
67 and DePaolo 1999, Chu et al., 2006, Hirata et al., 2008, Tacail et al., 2014, Heuser et  
68 al., 2016). This systematic and well-conserved offset argues in favor of a shared  
69 physiological effect on Ca isotope fractionation in mammal tissues. The depletion in  
70 heavy Ca isotopes is variable among organs, but taking blood as a baseline, Tacail et  
71 al. (2017b), based on a compilation of available data in mammals (Skulan and  
72 DePaolo 1999; Morgan et al. 2012; Tacail et al. 2014; Channon et al. 2015; and  
73 Heuser et al. 2016) on various organisms including humans, calculated a Ca isotopic  
74 offset  $\delta^{44/42}\text{Ca}$  between blood and diet of  $-0.30 \pm 0.13\text{‰}$  (1SD). The observed trophic

75 level effects in ecosystems could thus be explained by the propagation of this  
76 physiology-related isotopic fractionation from a trophic level to another.

77         Indeed, calcium isotope ratios were shown to decrease with trophic level  
78 position in marine ecosystems by Skulan et al. (1997) and this finding was later  
79 confirmed (Clementz et al. 2003; Martin et al., 2015; 2017b). Early work proposed a  
80 model to understand the relationship between dietary and mineralized calcium  
81 (Skulan and DePaolo, 1999) but subsequent studies raised some issues in interpreting  
82 calcium isotope values in terms of trophic fractionation, notably in terrestrial  
83 environments. Melin et al. (2014) studied calcium isotope ratios for terrestrial  
84 mammal ecosystems and concluded that while confirming the decrease in Ca isotope  
85 ratios in large carnivores, they also observed isotopic insensitivity to trophic levels  
86 between small faunivores and low trophic levels, suggesting limited applications of  
87 Ca isotopes in past ecosystems. Moreover the application of Ca isotopes for trophic  
88 level reconstruction in past continental ecosystems, including dinosaur fauna, was not  
89 conclusive (Heuser et al., 2011) although a recent study at regional scales permitted to  
90 distinguish between food sources between predatory dinosaurs (Hassler et al. 2018).  
91 Recent work offered encouraging perspectives in a Pleistocene mammalian fauna  
92 (Martin et al., 2017a) but some outliers remain difficult to interpret and may be so  
93 under the suspicion that physiological processes might be at play (Tacail et al. 2017a).  
94 Also, complexation of Ca with aqueous compounds (e.g. citrates, oxalates) potentially  
95 plays a role in isotopic fractionation between various plant or animal organs (Moynier  
96 and Fujii, 2017). Physiological differences have been previously discussed between  
97 fish and marine mammals (Martin et al. 2015) underlining the difficulty to interpret  
98 mammalian calcium isotope variability solely under the light of a trophic effect on

99 fractionation processes. Importantly, a comprehensive framework of Ca isotope  
100 distribution in modern terrestrial mammals is lacking.

101 In an effort to fill this gap, the present work reports Ca isotope ratios of  
102 modern enamel samples from the Tsavo National Park and from Turkana Basin  
103 (Kenya) (n = 64), and fossil enamel samples (n = 51) dated from *ca.* 4 Ma to 1.6 Ma  
104 from the Turkana Basin (Kenya). The  $^{44/42}\text{Ca}$  and  $^{43/42}\text{Ca}$  isotope ratios are compared  
105 with carbon isotope ( $^{13}\text{C}/^{12}\text{C}$ ), oxygen isotope ( $^{18}\text{O}/^{16}\text{O}$ ), strontium-calcium (Sr/Ca),  
106 and barium-calcium (Ba/Ca) ratios.

107

## 108 **2. Methods**

109

### 110 *2.1. Samples*

111

112 Tsavo National Park is situated in southern Kenya (*ca.* 3.4 S, 38.6 E, 550 m elevation)  
113 and has a mean annual temperature of 25 °C and 550 mm annual rainfall  
114 (Climatological Statistics for East Africa, 1975); it is a semi-desert bushland with  
115 riparian woodland (White, 1985). Samples of mammals were collected between 1997  
116 and 2011 and include the long-term collections at the Tsavo Research Center near  
117 Voi; samples in this collection date back to the 1960s. Fossil samples from the  
118 Turkana Basin were collected from the National Museums of Kenya and the Turkana  
119 Basin Institute. Ages of fossils are based on the stratigraphic and geochronologic  
120 work of Brown and McDougall (2011). Both modern and fossil materials were  
121 collected as part of a paleoecology project reported earlier (Cerling et al., 2015). For  
122 all samples, powdered enamel was collected using a low-speed dental drill.

123

124 2.2. Analytical techniques

125

126 We compared samples that had undergone the standard pre-treatment used in light  
127 stable isotope studies to remove organic matter and calcium carbonate (3% H<sub>2</sub>O<sub>2</sub>  
128 followed by 0.1 M acetic acid as in Passey et al, 2002). Samples were analyzed for  
129 δ<sup>13</sup>C and δ<sup>18</sup>O using digestion by 100% H<sub>3</sub>PO<sub>4</sub> and analyzed on an isotope ratio mass  
130 spectrometer using the standard ‰ notation where

131 
$$\delta^{13}\text{C}(\text{‰}) = (\text{R}_{\text{sample}}/\text{R}_{\text{standard}} - 1) * 1000 \quad (1)$$

132 where R<sub>sample</sub> and R<sub>standard</sub> are the <sup>13</sup>C/<sup>12</sup>C ratios in the sample and standard,  
133 respectively. An analogous equation defines δ<sup>18</sup>O. The isotope standard VPDB  
134 (Vienna-PDB) is used for both carbon and oxygen isotopes.

135 The remaining powdered samples were treated in the clean lab at LGLTPE,  
136 ENS de Lyon, France. For each dissolved sample, a fraction was taken for  
137 concentration analyses and another fraction was kept for purification of calcium.  
138 Concentration analyses were performed by means of inductively coupled plasma mass  
139 spectrometer (ICP-MS Agilent Technologies 7500 Series) for trace elements such as  
140 Sr, Ba, U, and major elements were measured on an inductively coupled plasma  
141 atomic emission spectrometer ICP-AES (Thermo electron corporation ICAP 6000).  
142 Measurements were controlled through a set of blanks and standards such as  
143 SRM1486. Calcium was purified following the protocol described in previous work  
144 using Eichrom Sr-specific resin (Sr-spec Eichrom®) and cation-exchange resin (AG-  
145 50WX-12) with ultrapure solutions of nitric and hydrochloric acids as elution agents  
146 (see details in Tacail et al. 2014; Martin et al. 2015; 2017a; 2017b). The purified  
147 fraction was measured for Ca isotopes on a Thermo Neptune Plus MC-ICPMS at  
148 medium resolution in static mode. Delta values were obtained using the standard

149 bracketing method using the *ICP Ca Lyon* standard issued from a Specpure calcium  
150 plasma standard solution (Alfa Aesar) (Tacaïl et al., 2014, 2016, 2017a; Martin et al.,  
151 2015, 2017a, 2017b; Hassler et al., 2018). SRM1486 was used as a secondary  
152 standard during each analytical sequence. Uncertainties are reported in Table S1 and  
153 represent 2 standard deviations of these analyses.  $\delta^{44/42}\text{Ca}$  values are defined as:  
154 
$$\delta^{44/42}\text{Ca}(\text{‰}) = \left( \frac{{}^{44}\text{Ca}/{}^{42}\text{Ca}_{\text{sample}}}{{}^{44}\text{Ca}/{}^{42}\text{Ca}_{\text{ICP Ca Lyon}}} - 1 \right) * 1000 \quad (2)$$
  
155 where  $\delta^{44/42}\text{Ca}$  is the normalized difference in per mil (‰) between a sample and our  
156 in-house *ICP Ca Lyon* standard. In this work, all measurements are expressed in  
157  $\delta^{44/42}\text{Ca}$  (Table S1) and we invite the reader to refer to supplementary material (Figure  
158 S1, Table S2) for details regarding conversions of data from the literature. Calcium  
159 isotope values are often expressed as  $\delta^{44/40}\text{Ca}$  values in the literature. As a guideline,  
160 the magnitude of variations of  $\delta^{44/42}\text{Ca}$  is almost exactly half that of  $\delta^{44/40}\text{Ca}$ .  
161 SRM1486 yielded a value of  $-1.047 \pm 0.013$  2SE ( $\pm 0.13$  2SD,  $n = 101$ ), which is  
162 undistinguishable from all SRM1486 samples measured at LGLTPE, with an average  
163 value of  $-1.024 \pm 0.006$  ‰ ( $n = 404$ , 2SE, Tacaïl et al., 2014, 2016, 2017a, Martin et  
164 al., 2015, 2017a, 2017b, Hassler et al., 2018) and reported  $\delta^{44/42}\text{Ca}$  values in 5 other  
165 studies ( $-1.009 \pm 0.026$ ‰, 2SE, Heuser and Eisenhauer 2008, Heuser et al. 2011,  
166 Heuser et al. 2016). More details on the compositions of reference materials are  
167 available in Table S2. All measured samples plotted in a  $\delta^{44/43}\text{Ca}$  versus  $\delta^{44/42}\text{Ca}$  space  
168 fall on a line with a slope of  $0.514 \pm 0.026$ , 2SE, in good agreement with the 0.5067  
169 slope predicted by the linear approximation of exponential mass-dependent  
170 fractionation (Fig. 1).

171

### 172 **3. Results**



173 Herbivores in both the modern and fossil samples range from browsers ( $\delta^{13}\text{C} < -8\text{‰}$ )  
174 to grazers ( $\delta^{13}\text{C} > -1\text{‰}$ ; see discussion in Cerling et al 2015); hippos are mixed  
175 feeders in this modern Tsavo ecosystem. For the Turkana Basin fossil dataset, the  
176 time span sampled is from *ca.* 4 to 1 Myr. A few taxa change their diets through this  
177 time period and some taxa at the genus level are present only in the fossil record. The  
178 elephantids *Loxodonta* and *Elephas* were grazers in the fossil record, but modern  
179 *Loxodonta* is a browser in modern ecosystems in East Africa (see Table S1 and S2  
180 and discussion in Cerling et al 1999, 2015) with *Elephas* being extinct in Africa  
181 today.

182 In the savanna mammals of the South African Kruger Park, Sponheimer and  
183 Lee-Thorp (2006) observed that grazers have higher Sr/Ca and Ba/Ca ratios than  
184 browsers. This observation is not confirmed here in the East African modern  
185 mammals of Tsavo (Fig S2). Noteworthy, we found that rhinos from this sample suite  
186 have extremely high Sr/Ca ratios with typical Sr contents that are one order of  
187 magnitude higher than in others animals (Fig S2). In agreement with the literature  
188 (Balter, 2004; Peek and Clementz, 2012), however, the Sr/Ca and Ba/Ca ratios are  
189 lower in carnivores than in herbivores in the modern dataset (Fig S2).

190 Fossil samples at Turkana are affected by diagenesis by the addition of trace  
191 metals: there is a strong positive correlation between Ba and Mn concentrations ( $R^2 =$   
192  $0.417, p^{***} < 10^{-5}$ ; Fig S4C; Table 1) and between Sr and U (U;  $R^2 = 0.247, p^{**} =$   
193  $0.0004$ ; Fig S4D; Table 1). As a consequence, the Sr/Ca and Ba/Ca ratios do not  
194 discriminate carnivores from herbivores in this particular fossil assemblage (Fig S3).  
195 In addition, the Sr/Ca and Ba/Ca ratios are correlated at Turkana ( $R^2=0.225, p^{**} =$   
196  $0.0008$ , Fig. S4B) while this correlation is not observed in the recent Tsavo fauna (Fig  
197 S4A).

198 That the Sr/Ca and Ba/Ca are correlated in fossil samples suggest a common  
199 diagenetic process for Sr and Ba. Likely, this diagenetic process involved the addition  
200 of a U and Mn-rich phase, which also contains Sr and Ba, explaining the overall  
201 increase by a factor of 1.7 and 3.3 of the Sr/Ca and Ba/Ca ratios, respectively,  
202 between modern and fossil samples. Mg/Ca ratios are not significantly different  
203 between modern and fossil samples. We conclude that our results show that diagenetic  
204 processes have altered the concentrations of Sr and Ba, and therefore the potential for  
205 isotopic alteration of the  $^{87}\text{Sr}/^{86}\text{Sr}$  ratio in fossil materials must be evaluated carefully.

206 Inversely, the relative sensitivity of trace and major elements to diagenesis can  
207 be used to ascertain that little or no diagenesis has occurred for major elements if the  
208 trace elements normalized to calcium show ratios similar to modern samples. This is  
209 most probably the case for South African Plio-Pleistocene fossils for which original  
210 Sr/Ca and Ba/Ca patterns are apparently preserved (Sponheimer et al., 2006; Balter et  
211 al., 2012).

212 The  $\delta^{44/42}\text{Ca}$  values range from  $-2.00\text{‰}$  to  $-0.98\text{‰}$  in the modern dataset of  
213 Tsavo/Turkana (Fig. 2A) and from  $-1.77\text{‰}$  to  $-0.94\text{‰}$  in the fossil dataset of Turkana  
214 (Fig. 3A). In both cases, carnivores exhibit the lowest  $\delta^{44/42}\text{Ca}$  values, but hippos also  
215 have quite low values, between hyenas and felids. Equids have  $\delta^{44/42}\text{Ca}$  values that  
216 fall in the variability of the felid carnivores, both in the modern and fossil datasets. In  
217 the modern dataset, suids exhibit similar  $\delta^{44/42}\text{Ca}$  values to equids, while fossils suids  
218 have relatively high  $\delta^{44/42}\text{Ca}$  values. Bovids, elephants and giraffes in the modern  
219 dataset have  $\delta^{44/42}\text{Ca}$  values more positive than equids, carnivores and hippos,  
220 although one equid outlier shows a  $\delta^{44/42}\text{Ca}$  value close to  $-1\text{‰}$ . The highest  $\delta^{44/42}\text{Ca}$   
221 values are from rhinos and some of the other herbivores such as one giraffe, one  
222 equid, a few elephants and bovids for the modern taxa analyzed (Fig. 2A). In the

223 fossil dataset, however, the fossil giraffes, bovids, rhinos and elephants have  
224 undistinguishable  $\delta^{44/42}\text{Ca}$  values (Fig. 3A).

225         Therefore, diagenesis appears to affect some trace elements (Ba, Mn, possibly  
226 Sr) but not for Ca-isotope ratios. The existence of a correlation between modern and  
227 fossil  $\delta^{44/42}\text{Ca}$  values (Fig. S5) implies that diagenesis of the Ca isotope ratios at  
228 Turkana is weak otherwise no correlation would have been obtained. Diagenesis of Ca  
229 isotopes is expected to be minimal in most cases, because phosphatic tissues are so  
230 rich in Ca that only extreme diagenesis (discussion above), which would modify the  
231 stoichiometry of CHA, would be able to overprint the original Ca isotope composition  
232 (Martin et al., 2017a).

233 **4. Discussion**

234 Recent data of calcium isotope compositions in enamel suggest a strong potential  
235 as a paleodietary indicator in marine settings (Skulan et al., 1997, Clementz et al.,  
236 2003; Martin et al., 2015; 2017b). On continents, however, data exhibit generally  
237 more complex patterning due, probably, to heterogeneous isotopic sources in soils and  
238 further fractionation in plants (Skulan and De Paolo, 1999; DePaolo 2004; Melin et  
239 al., 2014). Melin et al. (2014) analyzed the calcium isotope ratios of 21 bone samples  
240 from two modern mammalian communities in northern Borneo and northwestern  
241 Costa Rica: they observe a depletion of heavy calcium isotopes up the trophic chains  
242 involving two large vertebrate predators (one *Felis bengalensis* individual in Borneo  
243 and one *Panthera onca* individual in Costa Rica). Melin et al. (2014) concluded a lack  
244 of sensitivity of Ca isotopes to carnivory. Although tooth or bone samples from large  
245 predators are indeed difficult to secure, larger datasets including more of them are  
246 required to further explore this issue.

247 Our Ca isotope measurements arise from two modern datasets of mammals  
248 living at Tsavo National Park and at Turkana, both from Kenya; these datasets  
249 comprise 64 samples from individuals covering 9 different families of large mammals  
250 with 18 grazers, 21 browsers, 7 mixed feeders and 18 carnivores (Table 1). We  
251 considered several different digestive physiologies in the herbivore mammals of our  
252 dataset: ruminant foregut, non-ruminant foregut and hindgut. However, we found no  
253 statistically significant differences between groups. Although recent finds have  
254 highlighted that fractionation of calcium isotopes in the body mainly occurs from  
255 renal activity (Tacail et al. 2017b), it will be worth to expand the dataset and further  
256 explore potential links between digestive physiology and isotopic variability.  
257 Comparisons of  $\delta^{44/42}\text{Ca}$  values with respect to body mass are premature with our

258 current dataset; such studies should also include renal and digestive physiology as  
259 well as the C<sub>3</sub>/C<sub>4</sub> mix of diet while also comparing for body mass. Here, 1) we discuss  
260 a Trophic Level Effect (TLE) as recorded in tooth enamel of modern mammals,  
261 underlining significant differences in Ca and C isotope values between some  
262 carnivores and herbivores; 2) we highlight that variability in mammal resource use  
263 such as plants, soils and waters needs to be considered to account for the observed  
264 variability in Ca isotope values of their tissues and may be related to differences in  
265 calcium isotope ratios between grazers and browsers; and 3) we infer fossil mammal  
266 Ca isotopic ecology in light of the knowledge derived from the modern samples.

267

#### 268 4.1. $\delta^{44/42}\text{Ca}$ and the Trophic Level Effect (TLE) in modern mammals

269 Carnivores exhibit an important variability of the Ca isotope composition being the  
270 lightest samples of the dataset but also overlapping with herbivore Ca isotope values,  
271 except some of the very large herbivores, i.e. rhinos, giraffes and elephants (Fig. 2A).  
272 We report a carnivore-prey offset of 0.24‰ when considering all carnivores versus  
273 herbivores of the modern dataset, and an offset of 0.33‰ when considering *Panthera*  
274 *leo* and *Crocota crocuta* from Tsavo versus all modern herbivores. Therefore, a  
275 carnivore-prey offset of about 0.3‰ seems to characterize mammalian faunas. For the  
276 limited samples we have analyzed, the two modern felids from Tsavo, *Panthera leo* (n  
277 = 9) and *Panthera pardus* (n = 4) have differing  $^{44/42}\text{Ca}$  ratios, *P. leo* being the most  
278 depleted in heavy Ca isotopes ( $-1.63 \pm 0.09\text{‰}$ , 1SD) similarly to the single hyenid  
279 *Crocota crocuta* from Tsavo whereas *P. pardus* is enriched in heavy Ca isotopes  
280 ( $-1.46 \pm 0.16\text{‰}$ , 1SD). In the modern dataset from Turkana, *C. crocuta* (n = 2) is also  
281 the most depleted in heavy Ca but in this ecosystem, *P. leo* (n = 2) is notably enriched  
282 in heavy Ca ( $-1.18 \pm 0.01$ , 1SD), more so than *P. pardus* from Tsavo. Large

283 carnivores are flexible in their diet and their feeding habits may vary from one region  
284 to another. Considering only *P. leo* and *C. crocuta* at Tsavo, carnivores possess  
285 significant lower  $\delta^{44/42}\text{Ca}$  values than all herbivores, except the hippos (see discussion  
286 below). Bone is often a significant component of the diet of hyenids but also of *P. leo*.  
287 Across felid taxa, proportions of meat versus bone vary (Van Valkenburgh, 1996),  
288 indicating bone consumption needs to be considered as a non-negligible supplier of  
289 dietary calcium. Even a small amount of dietary bone ingested would shift the values  
290 toward light Ca (Heuser et al. 2011), and could explain the low  $\delta^{44/42}\text{Ca}$  values  
291 observed in our dataset for *P. leo* and *C. crocuta*. More calcium isotope data-points  
292 are needed to test for a potential isotope scattering among carnivores according to  
293 their feeding ecology. Based on behavioural observations, a dietary overlap exists  
294 between *C. crocuta* and *P. leo* (Hayward, 2006) and may help explain that both taxa  
295 display some of the most depleted Ca isotope values of the dataset. In the Pleistocene  
296 of France, *C. crocuta* possesses the most  $\delta^{44/42}\text{Ca}$ -depleted value of the dataset  
297 (Martin et al. 2017a), confirming our observations on *C. crocuta* from modern Kenya.

298         The  $\delta^{13}\text{C}$  distribution clearly distinguishes  $\text{C}_4$  from  $\text{C}_3$  trophic chains (Fig. 2B)  
299 and used with  $\delta^{44/42}\text{Ca}$  values provides further insights into niche partitioning.  
300 Browsing herbivores, composed of a few bovids, giraffes, rhinos and elephants  
301 exhibit high and low  $\delta^{44/42}\text{Ca}$  and  $\delta^{13}\text{C}$  values, respectively. They are separated in the  
302  $\delta^{44/42}\text{Ca}$  versus  $\delta^{13}\text{C}$  space from a group of predators, here represented by leopards,  
303 which show similar  $\delta^{13}\text{C}$  values but lower  $\delta^{44/42}\text{Ca}$  values (Fig. 2B). That *P. pardus*  
304 avoids prey living in open habitats has been reported in the wild (Hayward et al.  
305 2006b) and the isotopic distribution reported here indicates that some of the  
306 herbivores mentioned above, especially small bovids, could represent potential prey  
307 of the leopards. The preferred prey of the leopards have body masses not exceeding

308 25 kg (Hayward et al. 2006b) and therefore are not elephants, rhinos or giraffes.  
309 Further work is needed to sample and assess  $\delta^{44/42}\text{Ca}$  values for forest-dwelling small  
310 mammals such as small bovids (e.g., duikers, dik-diks, other neotragins) or primates,  
311 all of which are recognized prey of *P. pardus* and known to generally possess  
312 depleted  $\delta^{13}\text{C}$  values (around -12 to -15‰) (Cerling et al. 2004). On the other hand,  
313 another group of herbivores comprising most of the larger bovids, suids and equids  
314 occupy a distinct  $\delta^{13}\text{C}$  distribution indicating a  $\text{C}_4$  source for predators represented by  
315 *P. leo*, as indicated by their lower  $\delta^{44/42}\text{Ca}$  values, corresponding to the expected  
316 dietary shift in  $\delta^{44/42}\text{Ca}$  values between consumer and prey.

317 Hippos do not follow the trends observed in other herbivores and have very  
318 low  $\delta^{44/42}\text{Ca}$  values typical of carnivores. Such measurements are difficult to reconcile  
319 with a TLE given their known grazing ecology (Cerling et al. 2008); however, hippos  
320 are semi-aquatic and thus have different physiological adaptations than all the other  
321 non-aquatic mammals; influences on bone density and associated bone mass balance  
322 may affect their  $\delta^{44/42}\text{Ca}$  values. Although hippos have been occasionally observed to  
323 exhibit carnivory (Dudley et al. 2016) the observations are so sparse to suggest that  
324 carnivory is unlikely to have an observable Ca-isotope effect in hippos.

325

#### 326 *4.2. Ca isotope variability in environmental sources*

327

328 Drinking water represents a source of calcium for mammals with concentrations  
329 ranging between 15 and 150 ppm in modern-day streams (Tipper et al. 2016). Ca  
330 isotopes do not fractionate in a significant extent during geological processes leading  
331 to rather homogeneous isotope compositions in rocks, being sedimentary,  
332 metamorphic, plutonic or volcanic (Tipper et al., 2016). The Turkana modern and

333 fossil ecosystems are located around Lake Turkana and are comprised primarily of  
334 fluvial Quaternary sediments derived primarily from Ethiopian Tertiary and  
335 Quaternary volcanic rocks. The Tsavo ecosystem is located between Mombasa and  
336 Nairobi and consists of metamorphic basement in the east (all of Tsavo East NP and  
337 most of Tsavo West NP) with some Quaternary basalts in the western part of Tsavo  
338 West NP. If local Ca-isotope variations are found between different substrates,  
339 studies combining  $\delta^{44/42}\text{Ca}$  values with  $^{87}\text{Sr}/^{86}\text{Sr}$  may be useful to study fossil  
340 assemblages.

341         At the bottom of the trophic structure, mammalian herbivores source most of  
342 their calcium from plants. Contrary to geological processes, reviewing the literature  
343 shows that Ca isotopes fractionate in a significant extent between monocotyledons  
344 (including grasses) and leaves of dicotyledons (Fig. 4), thus representing an important  
345 source of isotopic variability. Roots of plants preferentially take up light Ca isotopes,  
346 and there is a further fractionation in favor of heavy isotopes with variable amplitude  
347 in leaves of dicotyledons, while this process is subdued or absent in monocotyledons  
348 (Cenki-Tok et al. 2009, Holmden and Bélanger 2010). This leads to a difference of  
349  $+0.31\text{‰}$  ( $p^{***} < 10^{-4}$ ) between whole monocotyledon plant tissue and the leaves of  
350 dicotyledons. This  $\delta^{44/42}\text{Ca}$  difference implies that grass and sedge consumers, i.e.  
351 grazers, should have a  $\delta^{44/42}\text{Ca}$  value lower by about 0.3‰ compared to the browsing  
352 leave-eaters; this is generally true for the modern Tsavo dataset (Fig. 2). If different  
353 plant parts (i.e., roots, shoots, leaves) have different  $\delta^{44/42}\text{Ca}$  values, those differences  
354 may be passed on to the consumer and this would be a useful tool for understanding  
355 fossil diet partitioning.

356         This recognized isotopic difference between plant types, being passed on to  
357 herbivores, eventually gets passed on to the next trophic level, i.e. carnivores. We



358 expect that carnivores feeding on grazers should exhibit different calcium isotopic  
359 compositions than carnivores feeding on browsers and this is supported by our  
360 modern dataset with lions and hyaenas showing more negative values ( $-1.65 \pm$   
361  $0.10\%$ , 1SD,  $n = 10$ ) than leopards ( $-1.46 \pm 0.16\%$ , 1SD,  $n = 4$ ).

362 Despite some scattering in  $\delta^{44/42}\text{Ca}$  values among predators, it becomes clear  
363 that in a modern ecosystem such as Tsavo, *P. pardus* feeds on prey with higher  
364  $\delta^{44/42}\text{Ca}$  values, and that *P. leo* and *C. crocuta* primarily feed on prey with lower  
365  $\delta^{44/42}\text{Ca}$  values. Remarkably, there is a tight  $\delta^{44/42}\text{Ca}$  versus  $\delta^{13}\text{C}$  clustering of all the  
366 taxa in the modern Tsavo panel, suggesting that Ca and C isotope ratios are driven, at  
367 least partially by common processes. The concomitant use of  $\delta^{44/42}\text{Ca}$  and  $\delta^{13}\text{C}$  values  
368 provides for the first time an encouraging perspective on carnivore niche partitioning  
369 between  $\text{C}_3$  and  $\text{C}_4$  prey. Certainly, more  $\delta^{44/42}\text{Ca}$  measurements covering specific  
370 feeding ecologies among modern felids are required to further discuss the use of  
371 calcium isotopes and decipher niche partitioning among large carnivores.

372

### 373 *4.3. Palaeoecological inferences using Ca isotopes*

374

375 The taxonomic distribution of the Ca isotope ratios have similar ordering for modern  
376 and fossil East African faunas (Fig. 2A and Fig. 3A). Comparing the  $\delta^{44/42}\text{Ca}$  values  
377 in modern Tsavo and fossil Turkana on a family taxon basis leads to a good  
378 correlation ( $R^2 = 0.621$ ,  $p^* = 0.012$ , Fig. 5) with an observed compression in the  
379  $\delta^{44/42}\text{Ca}$  range possibly due to differing feeding ecologies between fossil and modern  
380 analogues, as evidenced by high  $\delta^{44/42}\text{Ca}$  values for fossil suids and saber-tooth cats.

381 Plio-Pleistocene assemblages from Turkana in northern Kenya are from ca. 4.1  
382 Ma to 1.4 Ma, a period well after the rise of  $\text{C}_4$  ecosystems (Cerling et al., 1997), but

383 in a time where there were significant changes in dietary guilds represented in the  
384 fossil record (Cerling et al., 2015). The fossil Turkana ecosystem had similar  
385 taxonomic lineages as the modern Turkana ecosystem: bovids, elephantids, giraffids,  
386 equids, rhinocerotids. Fossil hyenids and felids were analyzed from Turkana; those  
387 fossil carnivora taxa include those with no modern analogues such as saber tooth  
388 felids.

389 The  $\delta^{44/42}\text{Ca}$  and  $\delta^{13}\text{C}$  relationships are preserved for some taxonomic groups,  
390 but not for all groups, when comparing the modern and fossil assemblages (Figure 2  
391 and Figure 3). Most taxonomic groups have similar rankings for  $\delta^{44/42}\text{Ca}$  for fossil  
392 versus modern samples (Figure 5) suggesting a conservative ecology and/or  
393 physiology. Although most taxonomic groups have similar  $\delta^{13}\text{C}$  values through time,  
394 some notable exceptions, such as elephantids and rhinocerotids, show similar  $\delta^{44/42}\text{Ca}$   
395 values in spite of differing  $\delta^{13}\text{C}$  values for the data considered here.

396 Bovids and equids have similar  $\delta^{13}\text{C}$  and  $\delta^{44/42}\text{Ca}$  values for both modern and  
397 fossil faunas although differences are noted. The fossil tragelaphins (*Taurotragus* and  
398 *Tragelaphus*) had higher grass components in their diets than the modern ones from  
399 Tsavo, and likewise the fossil alcelaphins (*Megalotragus*) had a slightly higher  
400 browse content than do modern alcelaphins from East Africa (see Cerling et al.,  
401 2015). Equids had similar  $\delta^{13}\text{C}$  values for both modern and fossil samples. Fossil and  
402 modern bovids have similar  $\delta^{44/42}\text{Ca}$  values, but modern equids have  $\delta^{44/42}\text{Ca}$  values  
403 slightly different than fossil equids.

404 The comparison between modern and fossil elephantids and rhinocerotids is  
405 noted here. Although the  $\delta^{44/42}\text{Ca}$  values are comparable, the diets of the studied  
406 samples are quite different, unlike all other fossil-modern comparisons in this study.  
407 Both elephantid fossil *Elephas* and *Loxodonta* were grazers, but modern *Loxodonta* is

408 primarily a browser (Cerling et al. 2015). The abundant fossil rhinocerotid  
409 *Ceratotherium* was a grazer and was analyzed as part of this study; the modern  
410 rhinocerotid *Diceros* was a browser (Cerling et al., 2015) and was analyzed as well.  
411 For these lineages,  $\delta^{44/42}\text{Ca}$  values are similar for fossil and modern comparisons, in  
412 spite of the dietary (grazing versus browsing) differences. Clearly, further  
413 comparison within the elephantid and rhinocerotids for both modern and fossil faunas  
414 is needed to understand why  $\delta^{44/42}\text{Ca}$  values in these groups appears to be  
415 conservative across dietary differences.

416 Modern suids, represented by *Phacochoerus aethiopicus*, have  $\delta^{44/42}\text{Ca}$  values  
417  $(-1.48 \pm 0.04\text{‰}, 1\text{SD}, n = 3)$  significantly different from fossil suids  $(-1.09 \pm 0.11\text{‰},$   
418  $1\text{SD}, n = 3)$ . The fossil dataset includes three genera (*Kolpochoerus*, *Metridiochoerus*  
419 and *Notochoerus*) and there is little variation in their respective Ca isotope values.

420 Modern *P. aethiopicus* are mostly herbivorous, feeding on grass. More specimens of  
421 fossil suids, especially contemporaneous lineages is needed to determine if Ca-  
422 isotopes can distinguish different feeding strategies, such as using underground  
423 storage organs, versus grass stems or leaves (Fig. 4).

424 It is noteworthy that the  $^{44}\text{Ca}$ -enrichment observed for carnivores between  
425 Turkana fossils and modern Tsavo samples is linked to five out of fourteen fossil  
426 samples (Fig. 5), with  $\delta^{44/42}\text{Ca}$  values above  $-1.2\text{‰}$ , which represent very high values  
427 even considering the modern Tsavo carnivores. Excluding these five samples, it can  
428 be noted that fossil and recent carnivores have identical  $\delta^{44/42}\text{Ca}$  values (Fig. 5)  
429 implying that those hyaenids and felids already occupied similar niches as modern *C.*  
430 *crocuta* and *P. leo*. There are no pure  $\text{C}_3$  carnivores in this dataset of fossil Turkana  
431 carnivores that fill the niche of extant leopards. All the fossil Turkana carnivores

432 examined in this paper relied on herbivores with a mixed C<sub>3</sub>-C<sub>4</sub> diet and cover a wide  
433 time range.

434 The group (n = 5) of fossil carnivores with extremely <sup>44</sup>Ca-enriched values  
435 (Fig. 3) includes four felids with two individuals of the genus *Dinofelis* (-1.17 ±  
436 0.10‰ and -1.03 ± 0.22‰), one machairodontid of the genus *Homotherium* (-1.08 ±  
437 0.15‰) and one indeterminate felid (-1.09 ± 0.12 ‰). Three of them are characterized  
438 by saber-shaped canines, the function of which has been interpreted to deliver a  
439 weaker bite force than *P. leo* (McHenry et al. 2007). According to our carbon isotope  
440 data, this group of felids fed on herbivores that consumed a mixture of C<sub>3</sub>-C<sub>4</sub> plants or  
441 the diet was a mix of grazers and browsers. The high δ<sup>44/42</sup>Ca values of Turkana  
442 saber-tooth cats imply an absence of bone consumption, probably reflecting  
443 adaptation to exclusive flesh-eating. Even considering such a derived feeding  
444 preference toward meat-based diet, the δ<sup>44/42</sup>Ca values for this group of felids remain  
445 high and applying an offset of about +0.3‰ (see 4.1) indicates a prey source with a  
446 δ<sup>44/42</sup>Ca enamel value around -0.8‰, i.e. not measured in our dataset. A provocative  
447 explanation would be that these carnivores relied mainly on an unanalyzed group of  
448 prey. As tempting as it may seem, two outliers may contradict such hypotheses and  
449 are represented by a machairodontine (saber-tooth) with low δ<sup>44/42</sup>Ca value (-1.53 ±  
450 0.12‰) as well as a hyenid with a particularly high δ<sup>44/42</sup>Ca value (-0.93 ± 0.13‰),  
451 both of which should be expected to respectively display high and low δ<sup>44/42</sup>Ca values  
452 instead. Alternatively, the model of Skulan and DePaolo (1999) could explain high  
453 δ<sup>44/42</sup>Ca values in some carnivores if a large proportion of ingested calcium ends up  
454 mineralized, in other words resulting in no fractionation between mineral and diet.  
455 Clearly, more data are needed to fully cover the range of δ<sup>44/42</sup>Ca variations in modern  
456 mammals, but the present study already gives encouraging grounds for first order

457 paleoecological reconstructions. Tighter time intervals for the fossil record would be  
458 beneficial for understanding past relationships in  $\delta^{44/42}\text{Ca}$  space, and additional studies  
459 of modern ecosystems are also needed.

460 **Acknowledgements**

461

462 We thank the Government of Kenya for permission to sample modern and fossil  
463 samples, the Kenya Wildlife Service for assistance in the field, and the National  
464 Museums of Kenya. Samples were collected with grants from the US National  
465 Science Foundation, the Packard Foundation, and the LSB Leakey Foundation. We  
466 also thank CNRS (Tellus-Rift) and ENS-Lyon for support of this project. We thank  
467 two anonymous reviewers for their insightful comments on the last version of this  
468 work.

469

470 **References**

471 Bagard, M.L., Schmitt, A.D., Chabaux, F., Pokrovsky, O.S., Viers, J., Stille, P.,  
472 Labolle, F. and Prokushkin, A.S., 2013. Biogeochemistry of stable Ca and radiogenic  
473 Sr isotopes in a larch-covered permafrost-dominated watershed of Central Siberia.  
474 *Geochimica et Cosmochimica Acta*, 114, 169-187.

475

476 Balter, V., Person, A., Labourdette, N., Drucker, D., Renard, M., & Vandermeersch,  
477 B. (2001). Les Néandertaliens étaient-ils essentiellement carnivores? Résultats  
478 préliminaires sur les teneurs en Sr et en Ba de la paléobiocénose mammalienne de  
479 Saint-Césaire. *Comptes Rendus de l'Académie des Sciences-Series IIA-Earth and*  
480 *Planetary Science*, 332(1), 59-65.

481

482 Balter, V. (2004). Allometric constraints on Sr/Ca and Ba/Ca partitioning in terrestrial  
483 mammalian trophic chains. *Oecologia*, 139(1), 83-88.

484

485 Balter, V., Braga, J., Télouk, P., & Thackeray, J. F. (2012). Evidence for dietary  
486 change but not landscape use in South African early hominins. *Nature*, 489(7417),  
487 558-560.  
488

489 Brown FH, Mcdougall I (2011) Geochronology of the Turkana depression of northern  
490 Kenya and southern Ethiopia. *Evolutionary Anthropology* 20.6: 217-227.

491 Cenko-Tok, B., Chabaux, F., Lemarchand, D., Schmitt, A. D., Pierret, M. C., Viville,  
492 D., Bagard, M.-L., & Stille, P. (2009). The impact of water–rock interaction and  
493 vegetation on calcium isotope fractionation in soil-and stream waters of a small,  
494 forested catchment (the Strengbach case). *Geochimica et Cosmochimica Acta*, 73(8),  
495 2215-2228.  
496

497 Cerling, T. E., Harris, J. M., MacFadden, B. J., Leakey, M. G., Quade, J., Eisenmann,  
498 V., & Ehleringer, J. R. (1997). Global vegetation change through the  
499 Miocene/Pliocene boundary. *Nature*, 389(6647), 153-158.  
500

501 Cerling TE, JM Harris, and MG Leakey (1999) Browsing and grazing in modern and  
502 fossil proboscideans. *Oecologia* 120: 364–374.

503 Cerling, T. E., Hart, J. A., Hart, T.B. 2004. Stable isotope ecology in the Ituri Forest.  
504 *Oecologia* 138:5–12.  
505

506 Cerling, T. E., Harris, J. M., Hart, J. A., Kaleme, P., Klingel, H., Leakey, M. G.,  
507 Levin, N.E. Lewison, R.L. & Passey, B. H. (2008). Stable isotope ecology of the  
508 common hippopotamus. *Journal of Zoology*, 276(2), 204-212.

509

510 Cerling TE, Andanje SA, Blumenthal SA, Brown FH, Chritz KL, Harris JM, Hart JA,  
511 Kirera FM, Kaleme P, Leakey LN, Leakey MG, Levin NE, Manthi FK, Passey BH,  
512 Uno KT (2015) Dietary changes of large herbivores in the Turkana Basin, Kenya  
513 from 4 to 1 million years ago. *Proceedings of the National Academy of Sciences*. 112:  
514 11467-11472.

515

516 Channon, M. B., Gordon, G. W., Morgan, J. L., Skulan, J. L., Smith, S. M., & Anbar,  
517 A. D. (2015). Using natural, stable calcium isotopes of human blood to detect and  
518 monitor changes in bone mineral balance. *Bone*, 77, 69-74.

519

520 Chu, N. C., Henderson, G. M., Belshaw, N. S., & Hedges, R. E. (2006). Establishing  
521 the potential of Ca isotopes as proxy for consumption of dairy products. *Applied*  
522 *geochemistry*, 21(10), 1656-1667.

523

524 Clementz, M. T., Holden, P., & Koch, P. L. (2003). Are calcium isotopes a reliable  
525 monitor of trophic level in marine settings?. *International Journal of*  
526 *Osteoarchaeology*, 13(1-2), 29-36.

527

528 Climatological Statistics for East Africa (1975) *Climatological Statistics for East*  
529 *Africa*. East African Meteorological Department, Nairobi.

530

531 DePaolo, D. J. (2004). Calcium isotopic variations produced by biological, kinetic,  
532 radiogenic and nucleosynthetic processes. *Reviews in mineralogy and geochemistry*,  
533 55(1), 255-288.



534

535 Dudley, J. P., Hang'Ombe, B. M., Leendertz, F. H., Dorward, L. J., Castro, J.,  
536 Subalusky, A. L., & Clauss, M. (2016). Carnivory in the common hippopotamus  
537 *Hippopotamus amphibius*: implications for the ecology and epidemiology of anthrax  
538 in African landscapes. *Mammal Review*, 46(3), 191-203.

539

540 Farkaš, J., Déjeant, A., Novák, M. and Jacobsen, S.B., 2011. Calcium isotope  
541 constraints on the uptake and sources of Ca<sup>2+</sup> in a base-poor forest: a new concept of  
542 combining stable ( $\delta^{44}/^{42}\text{Ca}$ ) and radiogenic ( $\epsilon\text{Ca}$ ) signals. *Geochimica et*  
543 *Cosmochimica Acta*, 75:7031-7046.

544

545 Gussone, N., and A. Heuser. "Biominerals and biomaterial." In *Calcium Stable*  
546 *Isotope Geochemistry*, pp. 111-144. Springer, Berlin, Heidelberg, 2016.

547

548 Hassler, A., Martin, J.E., Amiot, R., Tacail, T., Arnaud Godet, F., Allain, R., Balter,  
549 V. 2018. Calcium isotopes offer clues on resource partitioning among Cretaceous  
550 predatory dinosaurs. *Proceedings of the Royal Society B*. 285: 20180197.

551

552 Hayward, M. W. (2006). Prey preferences of the spotted hyaena (*Crocuta crocuta*) and  
553 degree of dietary overlap with the lion (*Panthera leo*). *Journal of Zoology*, 270(4),  
554 606-614.

555

556 Hayward, M. W., Henschel, P., O'brien, J., Hofmeyr, M., Balme, G., & Kerley, G. I.  
557 H. (2006b). Prey preferences of the leopard (*Panthera pardus*). *Journal of Zoology*,  
558 270(2), 298-313.  
559

560 Heuser, A., & Eisenhauer, A. (2008). The calcium isotope composition ( $\delta^{44}/^{40}\text{Ca}$ ) of  
561 NIST SRM 915b and NIST SRM 1486. *Geostandards and Geoanalytical Research*,  
562 32(3), 311-315.  
563

564 Heuser, A., Tütken, T., Gussone, N., & Galer, S. J. (2011). Calcium isotopes in fossil  
565 bones and teeth—Diagenetic versus biogenic origin. *Geochimica et Cosmochimica*  
566 *Acta*, 75(12), 3419-3433.  
567

568 Heuser, A., Eisenhauer, A., Scholz-Ahrens, K. E., & Schrezenmeir, J. (2016).  
569 Biological fractionation of stable Ca isotopes in Göttingen minipigs as a physiological  
570 model for Ca homeostasis in humans. *Isotopes in environmental and health studies*,  
571 52(6), 633-648.  
572

573 Heuser, A., A.-D. Schmitt, N. Gussone, and F. Wombacher. "Analytical methods." In  
574 *Calcium Stable Isotope Geochemistry*, pp. 23-73. Springer, Berlin, Heidelberg, 2016.  
575

576 Hindshaw, R. S., B. C. Reynolds, J. G. Wiederhold, M. Kiczka, R. Kretschmar, and  
577 B. Bourdon. (2013). Calcium isotope fractionation in alpine plants. *Biogeochemistry*  
578 112, no. 1-3:373-388.  
579

580 Hirata, T., Tanoshima, M., Suga, A., Tanaka, Y. K., Nagata, Y., Shinohara, A., &  
581 Chiba, M. (2008). Isotopic analysis of calcium in blood plasma and bone from mouse  
582 samples by multiple collector-ICP-mass spectrometry. *Analytical Sciences*, 24(11),  
583 1501-1507.

584

585 Holmden, C., & Bélanger, N. (2010). Ca isotope cycling in a forested ecosystem.  
586 *Geochimica et Cosmochimica Acta*, 74(3), 995-1015.

587

588 Martin, J. E., Tacail, T., Adnet, S., Girard, C., & Balter, V. (2015). Calcium isotopes  
589 reveal the trophic position of extant and fossil elasmobranchs. *Chemical Geology*,  
590 415, 118-125.

591

592 Martin, J. E., Tacail, T., & Balter, V. (2017a). Non-traditional isotope perspectives in  
593 vertebrate palaeobiology. *Palaeontology*. 60 :485–502.

594

595 Martin, J. E., Vincent, P., Tacail, T., Khaldoune, F., Jourani, E., Bardet, N., & Balter,  
596 V. (2017b). Calcium Isotopic Evidence for Vulnerable Marine Ecosystem Structure  
597 Prior to the K/Pg Extinction. *Current Biology*. 27: 1641-1644.

598

599 McHenry, C.R., Wroe, S., Clausen, P.D., Moreno, K., Cunningham, E. 2007.  
600 Supermodeled sabercat, predatory behavior in *Smilodon fatalis* revealed by high-  
601 resolution 3D computer simulation. *Proceedings of the National Academy of Sciences*.  
602 104: 16010-16015.

603

604 Melin, A. D., Crowley, B. E., Brown, S. T., Wheatley, P. V., Moritz, G. L., Yu, Y.,  
605 Bernard, H., DePaolo, D.J., Jacobson, A.D. & Dominy, N. J. (2014). Calcium and  
606 carbon stable isotope ratios as paleodietary indicators. *American journal of physical*  
607 *anthropology*, 154(4), 633-643.

608

609 Moore, J., Jacobson, A.D., Holmden, C. and Craw, D., 2013. Tracking the  
610 relationship between mountain uplift, silicate weathering, and long-term CO<sub>2</sub>  
611 consumption with Ca isotopes: Southern Alps, New Zealand. *Chemical Geology*,  
612 341,110-127.

613

614 Morgan, J. L., Skulan, J. L., Gordon, G. W., Romaniello, S. J., Smith, S. M., &  
615 Anbar, A. D. (2012). Rapidly assessing changes in bone mineral balance using natural  
616 stable calcium isotopes. *Proceedings of the National Academy of Sciences*, 109(25),  
617 9989-9994.

618

619 Moynier, F., and T. Fujii. (2017). Calcium isotope fractionation between aqueous  
620 compounds relevant to low-temperature geochemistry, biology and medicine. *Scientific*  
621 *Reports*, 7, 44255.

622

623 Page, B., D., Thomas D. Bullen, and Myron J. Mitchell. (2008). Influences of calcium  
624 availability and tree species on Ca isotope fractionation in soil and vegetation.  
625 *Biogeochemistry* 88, no:1-13.

626

627 Passey BH, ME Perkins, MR Voorhies, TE Cerling, JM Harris, and ST Tucker, 2002,  
628 Timing of C<sub>4</sub> biomass expansion and environmental change in the Great Plains: an  
629 isotopic record from fossil horses. *Journal of Geology* 110: 123–140.

630

631 Peek, S., & Clementz, M. T. (2012). Sr/Ca and Ba/Ca variations in environmental and  
632 biological sources: A survey of marine and terrestrial systems. *Geochimica et*  
633 *Cosmochimica Acta*, 95, 36-52.

634

635 Reynard, L. M., Henderson, G. M., & Hedges, R. E. M. (2010). Calcium isotope  
636 ratios in animal and human bone. *Geochimica et Cosmochimica Acta*, 74(13), 3735-  
637 3750.

638

639 Reynard, L. M., Henderson, G. M., & Hedges, R. E. M. (2011). Calcium isotopes in  
640 archaeological bones and their relationship to dairy consumption. *Journal of*  
641 *Archaeological Science*, 38(3), 657-664.

642

643 Reynard, L. M., Pearson, J. A., Henderson, G. M., & Hedges, R. E. M. (2013).  
644 Calcium isotopes in juvenile milk-consumers. *Archaeometry*, 55(5), 946-957.

645

646 Reynard, B., & Balter, V. (2014). Trace elements and their isotopes in bones and  
647 teeth: Diet, environments, diagenesis, and dating of archeological and paleontological  
648 samples. *Palaeogeography, Palaeoclimatology, Palaeoecology*, 416, 4-16.

649

650 Russell, W. A., & Papanastassiou, D. A. (1978). Calcium isotope fractionation in ion-  
651 exchange chromatography. *Analytical Chemistry*, 50(8), 1151-1154.

652

653 Schmitt, A.D., Chabaux, F. and Stille, P., (2003). The calcium riverine and  
654 hydrothermal isotopic fluxes and the oceanic calcium mass balance. *Earth and*  
655 *Planetary Science Letters*, 213, 503-518.

656

657 Skulan, J., DePaolo, D. J., & Owens, T. L. (1997). Biological control of calcium  
658 isotopic abundances in the global calcium cycle. *Geochimica et Cosmochimica Acta*,  
659 61(12), 2505-2510.

660

661 Skulan, J., & DePaolo, D. J. (1999). Calcium isotope fractionation between soft and  
662 mineralized tissues as a monitor of calcium use in vertebrates. *Proceedings of the*  
663 *National Academy of Sciences*, 96(24), 13709-13713.

664

665 Sponheimer, M., & Lee-Thorp, J. A. (2006). Enamel diagenesis at South African  
666 Australopith sites: Implications for paleoecological reconstruction with trace  
667 elements. *Geochimica et Cosmochimica Acta*, 70(7), 1644-1654.

668

669 Tacail, T., Albalat, E., Télouk, P., & Balter, V. (2014). A simplified protocol for  
670 measurement of Ca isotopes in biological samples. *Journal of Analytical Atomic*  
671 *Spectrometry*, 29(3), 529-535.

672

673 Tacail, T., Télouk, P., & Balter, V. (2016). Precise analysis of calcium stable isotope  
674 variations in biological apatites using laser ablation MC-ICPMS. *Journal of*  
675 *Analytical Atomic Spectrometry*, 31(1), 152-162.

676

677 Tacail T, Thivichon-Prince B, Martin JE, Charles C, Viriot L, Balter V. 2017a.

678 Assessing human weaning practices with calcium isotopes in tooth enamel.

679 *Proceedings of the National Academy of Sciences*. 27: 1641–1644.

680 Tacail T, Balter V, Pelletier S, Barbesier M, Hernandez J-A, Jaouen K, Lafage-

681 Proust M-H, Lamboux A, Soulage C, Télouk P, Wegrzyn J, Albarède F & Fouque D.

682 2017b. A Comprehensive Box-Model for Calcium Isotopes in Humans. Goldschmidt

683 Conference, August 13-18, Paris.

684 Tipper, E. T., Schmitt, A. D., Gussone, N. (2016). Global Ca Cycles: Coupling of

685 Continental and Oceanic Processes. In *Calcium Stable Isotope Geochemistry* (pp.

686 173-222). Springer Berlin Heidelberg.

687

688 Valdes, M. C., Moreira, M., Foriel, J., Moynier, F. (2014). The nature of Earth's

689 building blocks as revealed by calcium isotopes. *Earth and Planetary Science Letters*,

690 394:135–145.

691

692 Van Valkenburgh, B. 1996. Feeding behavior in free-ranging, large African

693 carnivores. *Journal of Mammalogy*. 77:240–254.

694

695 White F (1983) *The vegetation of Africa: a descriptive memoir to accompany the*  
696 *UNESCO/AETFAT/UNSO vegetation map of Africa by F White*. Natural Resources  
697 Research Report XX, UNESCO, Paris, France.

698 Wiegand, B.A., Chadwick, O.A., Vitousek, P.M. and Wooden, J.L., 2005. Ca cycling  
699 and isotopic fluxes in forested ecosystems in Hawaii. *Geophysical Research Letters*,  
700 32(11).

701

702 Wieser, M. E., Buhl, D., Bouman, C., & Schwieters, J. (2004). High precision calcium  
703 isotope ratio measurements using a magnetic sector multiple collector inductively  
704 coupled plasma mass spectrometer. *Journal of Analytical Atomic Spectrometry*, 19(7),  
705 844-851.

706

707

708 **Figure captions.**

709 **Figure 1.** Three-isotope-plot for all data measured in this study, with  $\delta^{43/42}\text{Ca}$  (‰) as  
710 a function of  $\delta^{44/42}\text{Ca}$  (‰) relative to *ICP Ca Lyon* bracketing standard. The samples  
711 and standards fall on a line with a slope of  $0.518 \pm 0.028$  (2SE), indistinguishable  
712 from the 0.507 slope predicted by the exponential mass-dependent fractionation law  
713 (red stippled line). Error bars correspond to 2SD. The blue line corresponds to the  
714 regression line. The red shaded area corresponds to the 95% confidence interval on  
715 the regression line.

716

717 **Figure 2. A,**  $\delta^{44/42}\text{Ca}$  variability by taxonomic groups (‰, rel. *ICP Ca Lyon*),  
718 arranged by increasing average values, as measured in tooth enamel of a mammalian  
719 assemblage from the modern ecosystem of Tsavo, Kenya. **B,**  $\delta^{44/42}\text{Ca}$  as a function of



720  $\delta^{13}\text{C}$  measured from tooth enamel from the same modern assemblage. Note the spatial  
721 distinction between Hyenidae + *P. leo* and *P. pardus*. Abbreviations: t, tragelaphine  
722 bovids.

723

724 **Figure 3. A**, Calcium isotope variability by taxonomic grouping of fossil assemblage  
725 of Turkana Basin, Kenya. **B**,  $\delta^{44/42}\text{Ca}$  as a function of  $\delta^{13}\text{C}$  measured from tooth  
726 enamel from the same fossil assemblage. Abbreviations: a, alcelaphine bovids.

727

728 **Figure 4.** Calcium isotope variability compared between soils, browser and grazer  
729 tooth enamel and their potential source foods, i.e. plant parts including roots, shoots,  
730 leaves/fruits and whole Poacea (data for soils and plants derived from Bagard et al.  
731 2013; Chu et al. 2006; Farkas et al. 2011; Gussone and Heuser, 2016; Heuser et al.,  
732 2016; Hindshaw et al. 2013; Holmden et al. 2010; Moore et al. 2013; Page et al. 2008;  
733 Schmitt et al. 2003; Skulan and DePaolo, 1999; Tacail et al. 2014; Wiegand et al.  
734 2005). Student t-test P values are indicated: \*\*P = 0.001–0.01; and \*\*\*P<0.001.

735

736 **Figure 5.**  $\delta^{44/42}\text{Ca}$  in fossil tooth enamel from Turkana Basin compared to  $\delta^{44/42}\text{Ca}$  of  
737 modern tooth enamel from Tsavo for similar taxonomic groups.

738

739

740

741

742

743

744

745

746

747

748

749

750

751

752

753

754

755

756

757

758

759

760

761

762

763

764

765

766

767

768

769

770 **Supplementary data**

771

772 **Conversion of literature data to ICP Ca Lyon**

773 All standards and datasets from the literature expressed in  $\delta^{44/40}\text{Ca}$  values were  
774 converted to  $\delta^{44/42}\text{Ca}$  by dividing by 2.048, as calculated using the exponential mass-  
775 dependent fractionation law (e.g. Russell et al., 1978, Maréchal et al., 1999).

776

777 The measured  $\delta^{44/42}\text{Ca}$  values of 4 international Ca isotope standards expressed with  
778 respect to SRM915a standard were compared to 71 values from the literature as  
779 compiled from 52 publications. The constant difference of  $-0.518 \pm 0.025$  ‰  
780 between standards measured against SRM915a *versus* ICP Ca Lyon (Figure S1) was  
781 used to calculate the corresponding isotope compositions of international standards  
782 from the literature with respect to *ICP Ca Lyon*, as well as to compare our dataset to  
783 literature dataset published against SRM915a, Seawater, SRM915b, SRM1486, CaF2  
784 GEOMAR, BSE and the CaCO3 standard described in Skulan et al. (1997). All the  
785 measured and compiled  $\delta^{44/42}\text{Ca}$  values of Ca standards and reference materials are  
786 summarized in Table S2.

787

788 **Table S1.** Modern and fossil samples analyzed in this study for calcium isotope  
789 values (expressed as  $\delta^{44/42}\text{Ca}$  and  $\delta^{43/42}\text{Ca}$  in ‰ relative to standard ICP Ca-Lyon),  
790 carbon and oxygen isotope values as well as concentrations and concentration ratios  
791 for some major and trace elements.

792

793 **Table S2.** Table summarizing the isotope compositions of all 7 standards or reference  
794 materials measured or converted to *ICP Ca Lyon*. Underlined values are the values

795 used to convert literature datasets from a given reference material to ICP Ca Lyon  
796 when necessary.

797

798 **Supp. Figure 1.** Literature  $\delta^{44/42}\text{Ca}$  average values (‰, rel. *SRM915a*) as a function of  
799 measured  $\delta^{44/42}\text{Ca}$  average values (‰, rel. *ICP Ca Lyon*) of 4 international Ca isotope  
800 standards (Seawater, SRM915a, SRM915b and SRM1486). This value is thus used to  
801 convert literature datasets expressed against *SRM915a* to *ICP Ca Lyon*. The blue line  
802 is the regression line for which the equation is given in blue. The dotted line is the  
803 identity line ( $y = x$ ); the dotted grey line is the line with slope 1 and y-intercept of  
804 0.518‰. The 0.518‰ value is the one used for conversions of datasets initially  
805 expressed relative to SRM915a. Error bars are 2SE (95% confidence interval from the  
806 Student's t-test).

807

808 **Supp. Figure 2.** Log<sub>10</sub>(Sr/Ca) ratios in the modern mammal assemblage of Tsavo,  
809 Kenya represented by **A**, family groups and by **B**, ecological groups. Log<sub>10</sub>(Ba/Ca)  
810 ratios in the modern mammal assemblage of Tsavo, Kenya represented by **C**, family  
811 groups and by **D**, ecological groups.

812

813 **Supp. Figure 3.** **A**, Log<sub>10</sub>(Sr/Ca) and **B**, Log<sub>10</sub>(Ba/Ca) ratios in the fossil mammal  
814 assemblage of Turkana Basin, Kenya represented by family.

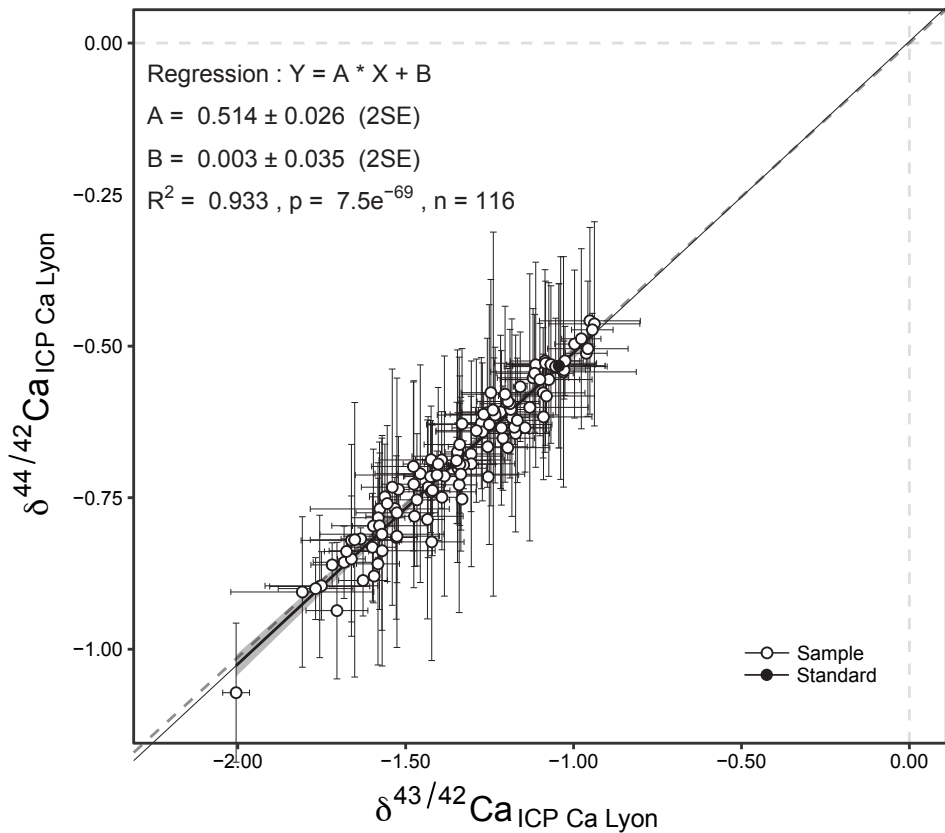
815

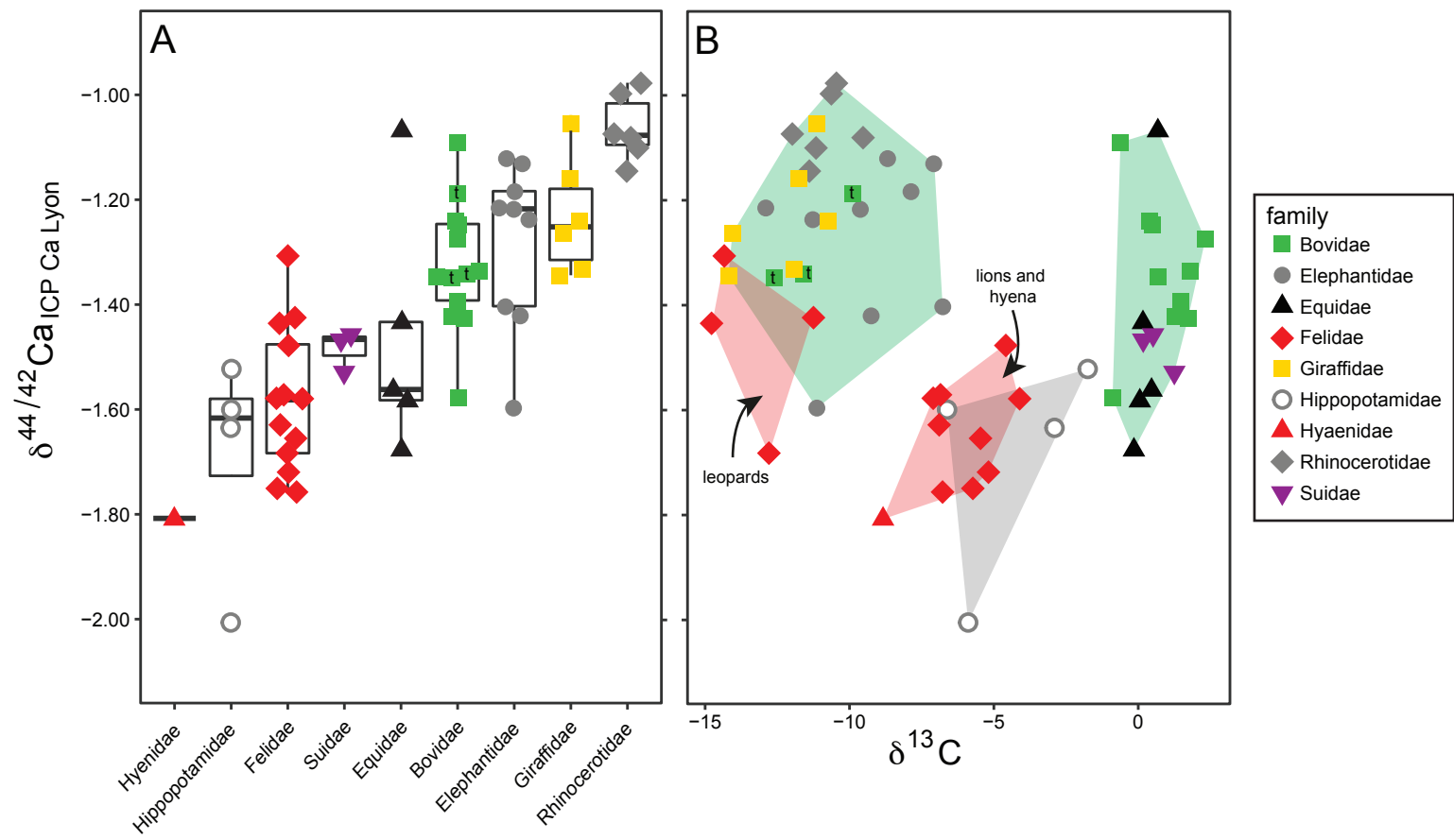
816 **Supp. Figure 4.** Trace element concentrations measured from tooth enamel samples  
817 from modern and fossil mammals analyzed in this study. Green corresponds to  
818 herbivores and red corresponds to carnivores. **A**, Ba/Ca ratios as a function of Sr/Ca  
819 ratios from the modern mammalian assemblage; **B**, Ba/Ca ratios as a function of

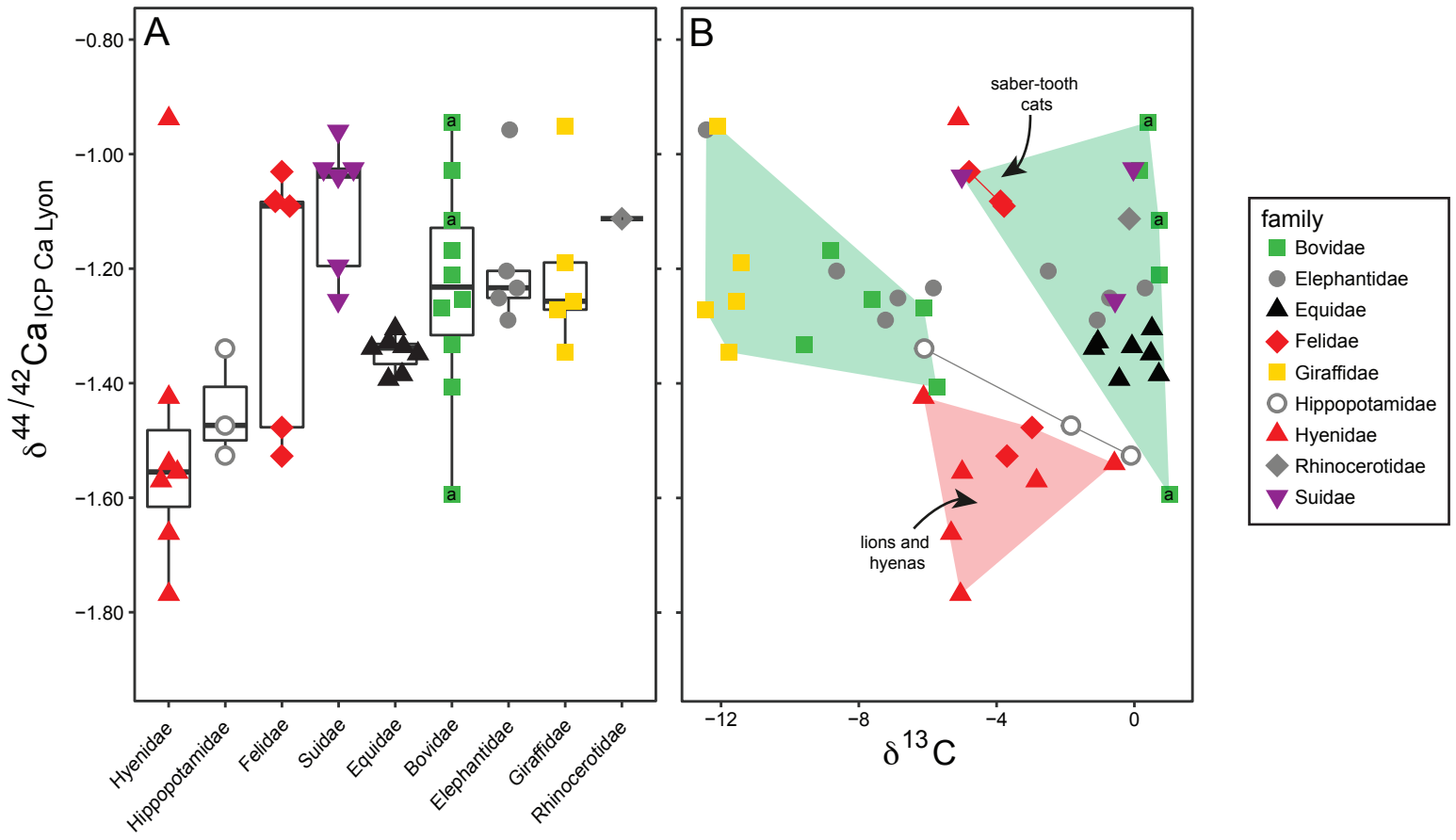
820 Sr/Ca ratios from the fossil mammalian assemblage of Turkana Basin; **C**, Mn as a  
821 function of Ba from the fossil mammalian assemblage of Turkana Basin; **D**, U as a  
822 function of Sr from the fossil mammalian assemblage of Turkana Basin.

823

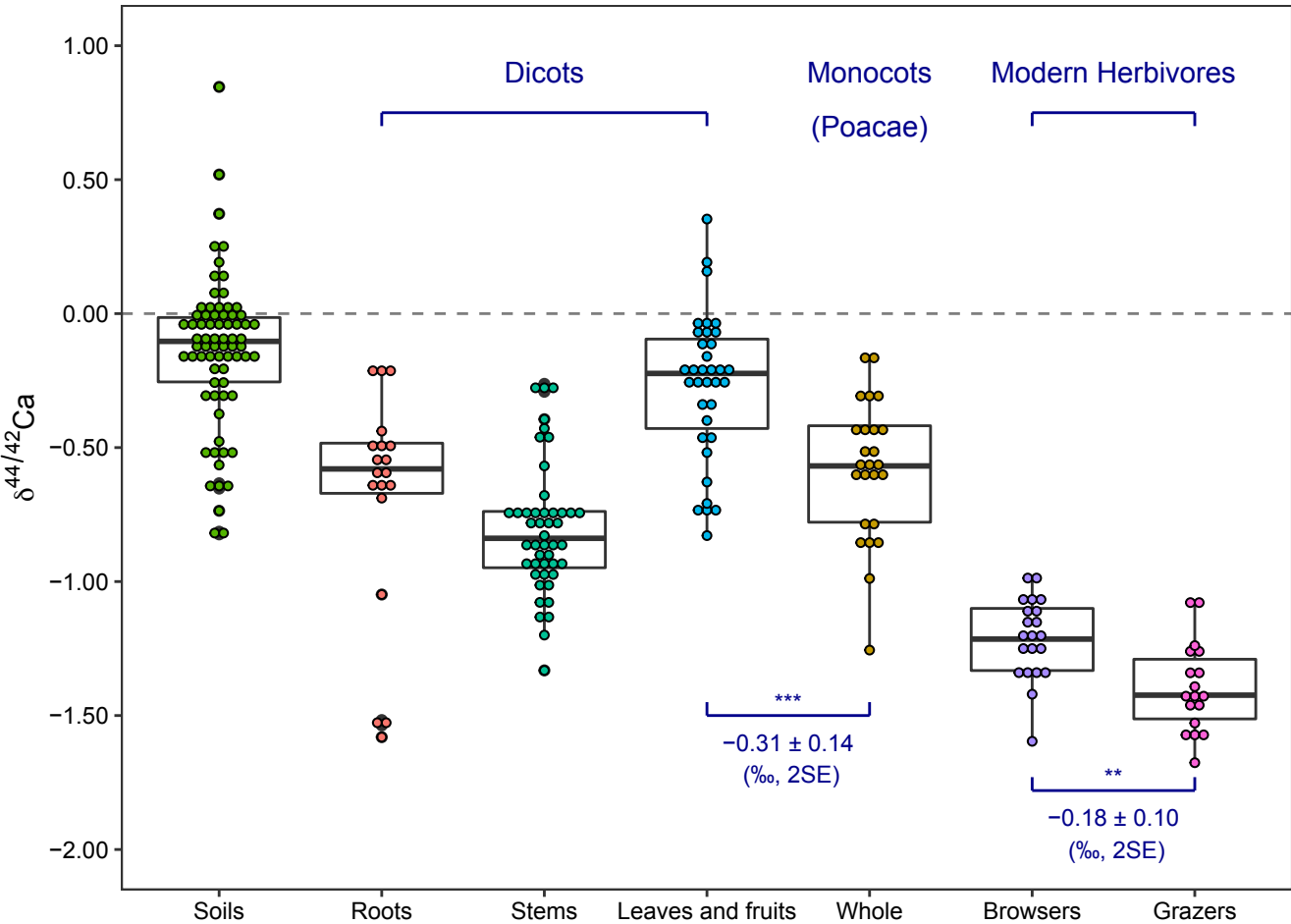
824 **Supp. Figure 5.** Comparison of  $\delta^{44/42}\text{Ca}$  values measured on pairs of treated versus  
825 untreated samples (in ‰, relative to *ICP Ca Lyon* standard). The blue line is the  
826 identity line. Error bars are 2SD.

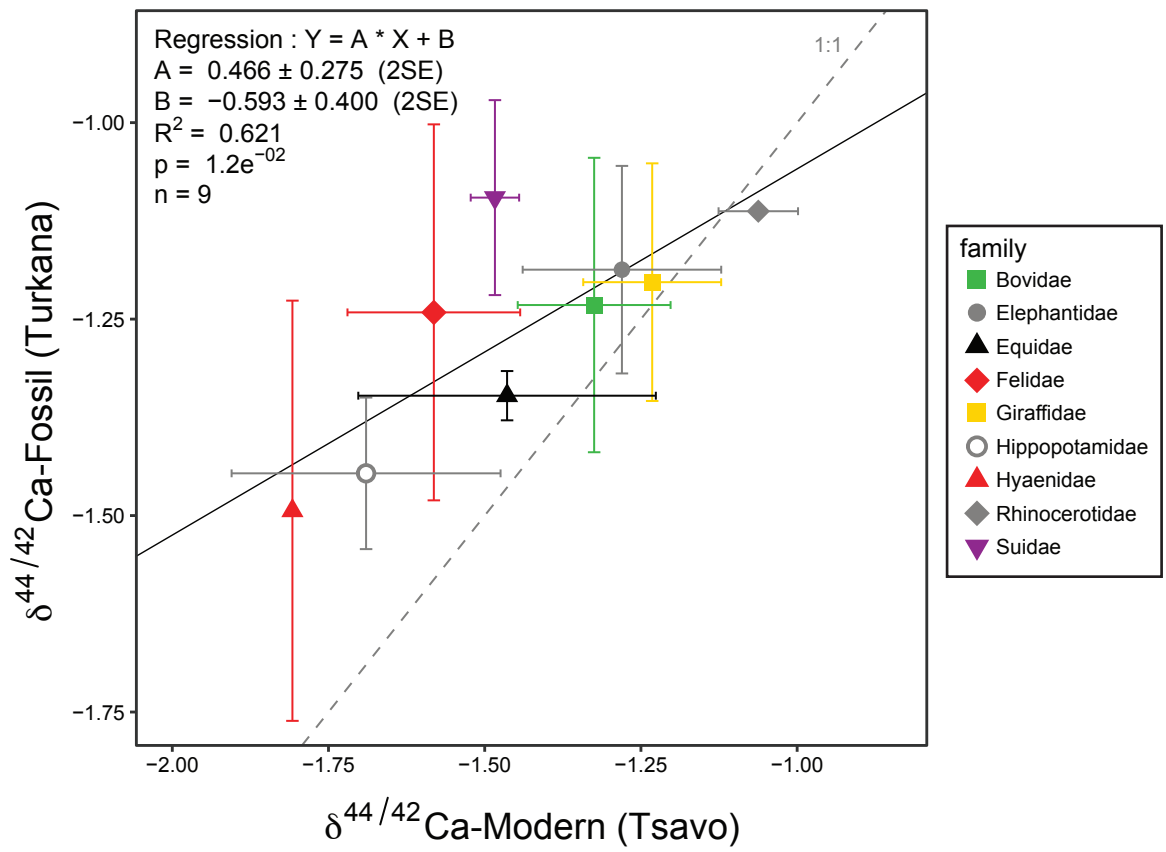












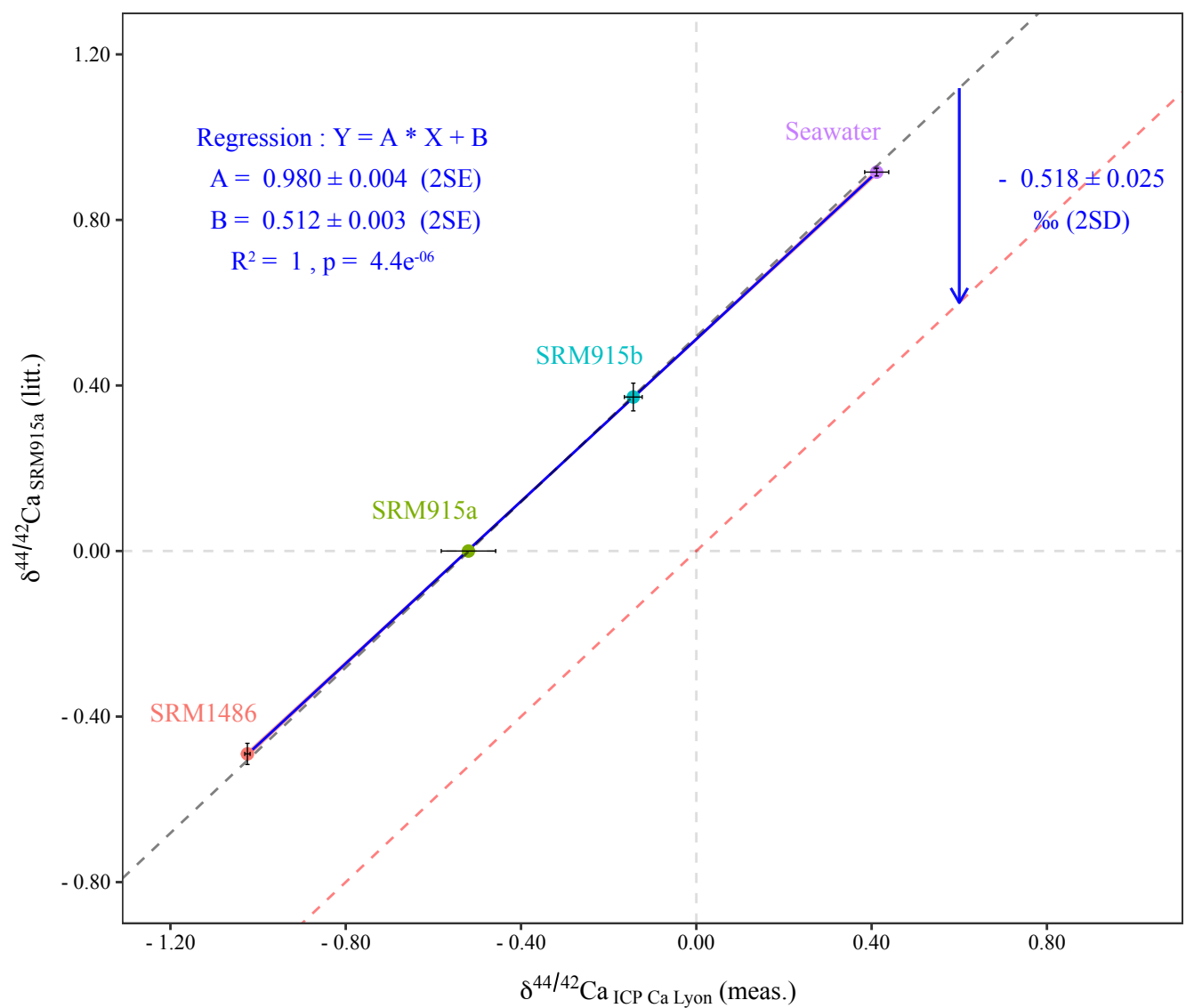
TSAVO\_TURKANA

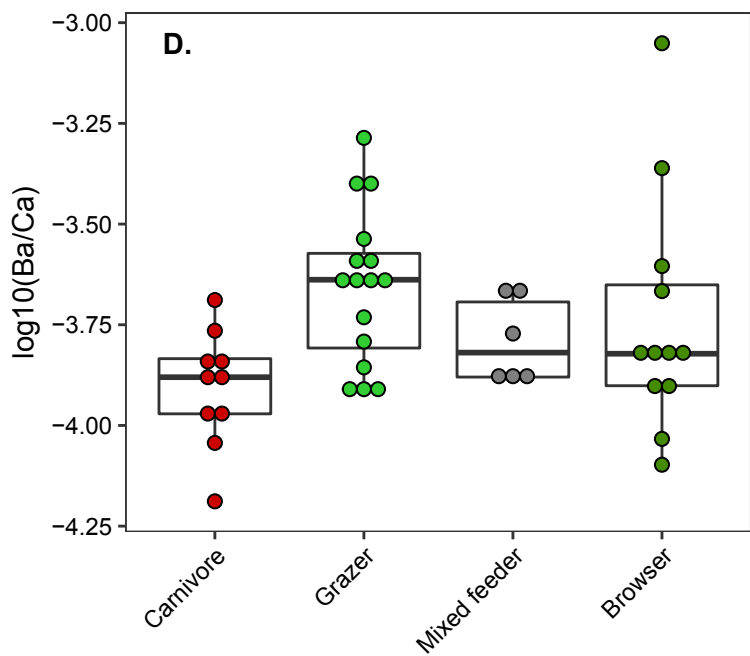
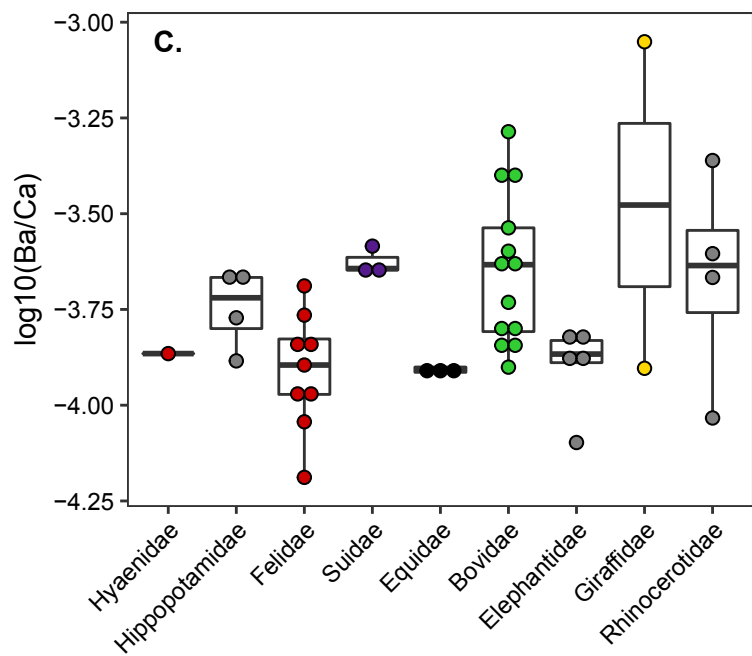
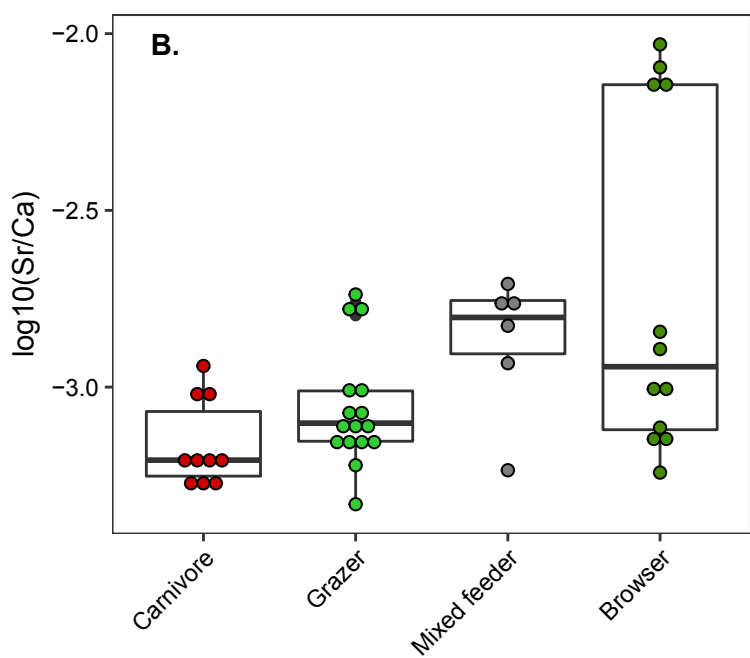
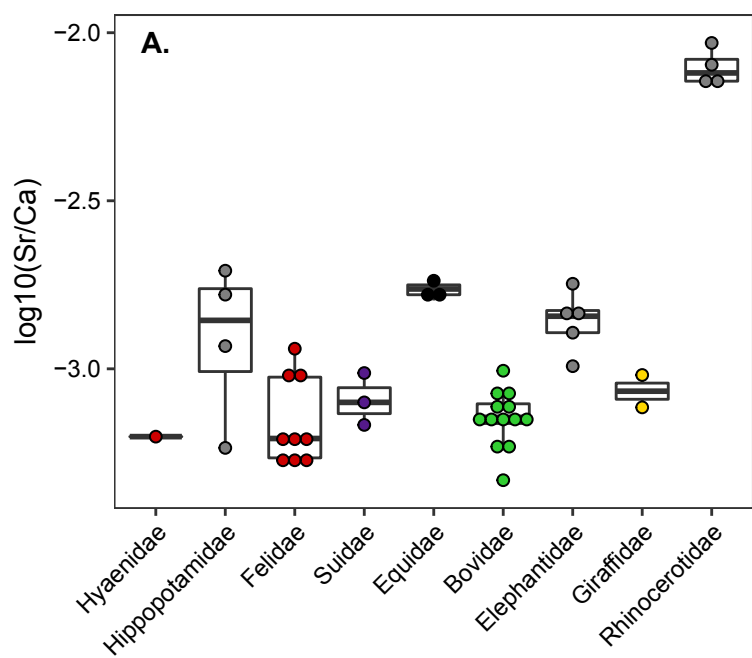
Table with columns: family, genus\_species, DIGESTIVE PHYSIOLOGY, ecology, MOD\_FOSS, sample\_id, treat, unseal, genot\_fm, DATE, MY\_BIAGE, RANGE, tooth\_type, 618C, 618D, 644zCa (%), 2SD, 644zCa (%), 2SD, 644zCa (%), 2SD, 644zCa (%), 2SD, Ca/P, Mg/Ca (AS), S/Ca, Ba/Ca, Cu (%), Mn (ppm), U (ppm). Rows include various species like Rhinocerotidae, Giraffidae, Equidae, Bovidae, Hippopotamidae, etc.

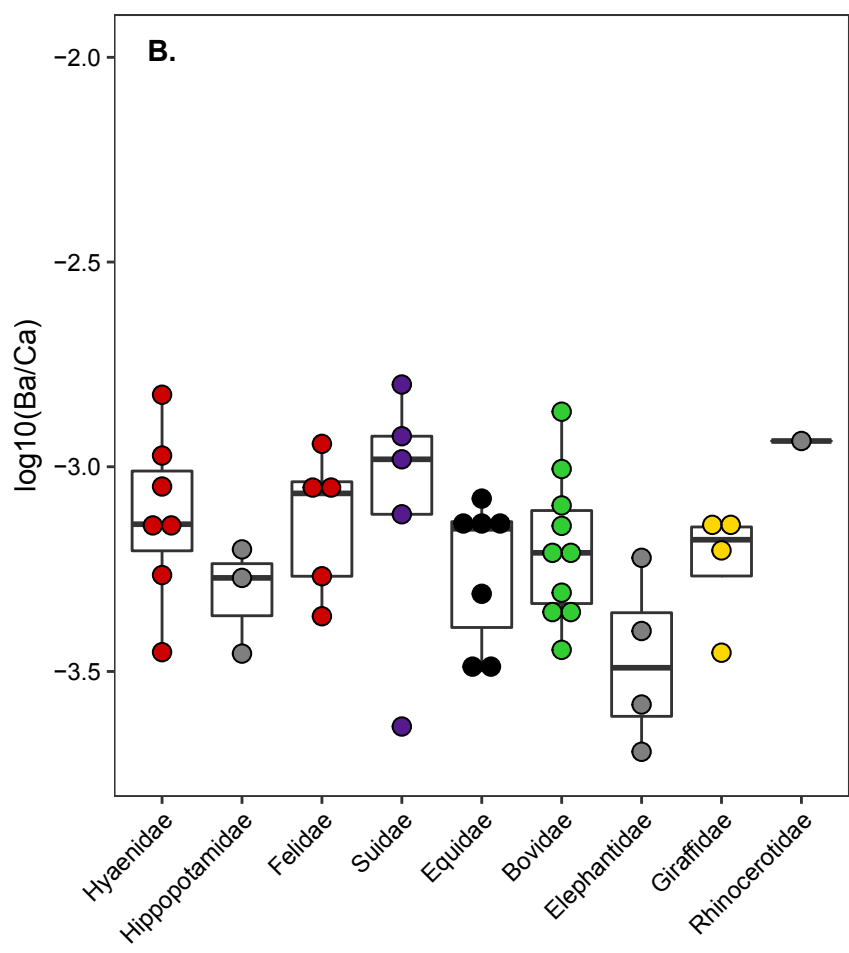
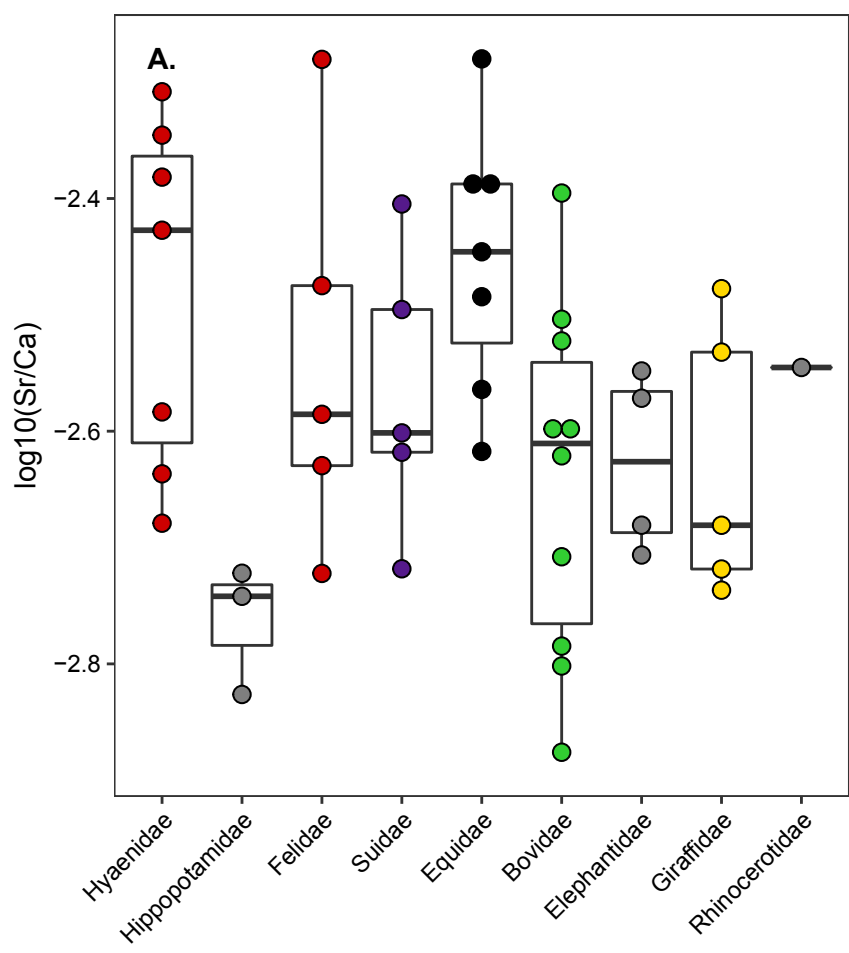
Standard as sample	Method	n	$\delta^{44/42}\text{Ca}$ (‰)		$\delta^{44/42}\text{Ca}$ (‰)		Conv. to ICP Ca Lyon by adding :	References	
			rel. ICP Ca Lyon	2SD	2SE	rel. Literature Ref. Mat.			
Seawater	Measured	17 meas.	<b>0.412</b>	0.107	0.027	-	-	32, 51, 52	
	Converted	39 refs.	<b>0.397</b>	0.057	0.009	<b>0.916</b>	rel. SRM915a	-0.518	1-5, 8-11, 13, 20-30, 36, 40, 41, 43, 44, 45, 49, 50, 54, 55, 57, 59
SRM915b	Measured	26 meas.	<b>-0.144</b>	0.101	0.020	-	-	32, 51-53	
	Converted	7 refs.	<b>-0.146</b>	0.073	0.034	<b>0.372</b>	rel. SRM915a	-0.518	6, 11, 15, 20, 40, 42, 58
SRM915a	Measured	5 meas.	<b>-0.520</b>	0.100	0.062	-	-	53	
	Used for conversion	-	<b>-0.518</b>	-	-	<b>0.000</b>	rel. SRM915a	-0.518	-
SRM1486	Measured	101 meas.	<b>-1.047</b>	0.130	0.013	-	-	This study	
	Measured	404 meas.	<b>-1.024</b>	0.125	0.006	-	-	14, 33-34, 51-53	
	Converted	5 refs.	<b>-1.009</b>	0.041	0.026	<b>-0.490</b>	rel. SRM915a	-0.518	15, 18, 19, 31
CaF2 GEOMAR	Converted	13 refs.	<b>0.180</b>	0.041	0.013	<b>0.698</b>	rel. SRM915a	-0.518	5, 12, 13, 16, 17, 22, 36, 39, 44, 45, 54
BSE	Converted	5 refs.	<b>-0.036</b>	0.021	0.013	<b>0.482</b>	rel. SRM915a	-0.518	7, 35, 37, 38, 46
CaCO3 (Skulan et al. 1997)	Converted	2 refs.	<b>-0.023</b>	0.041	NA	<b>-0.435</b>	rel. Seawater	+0.412	47, 48

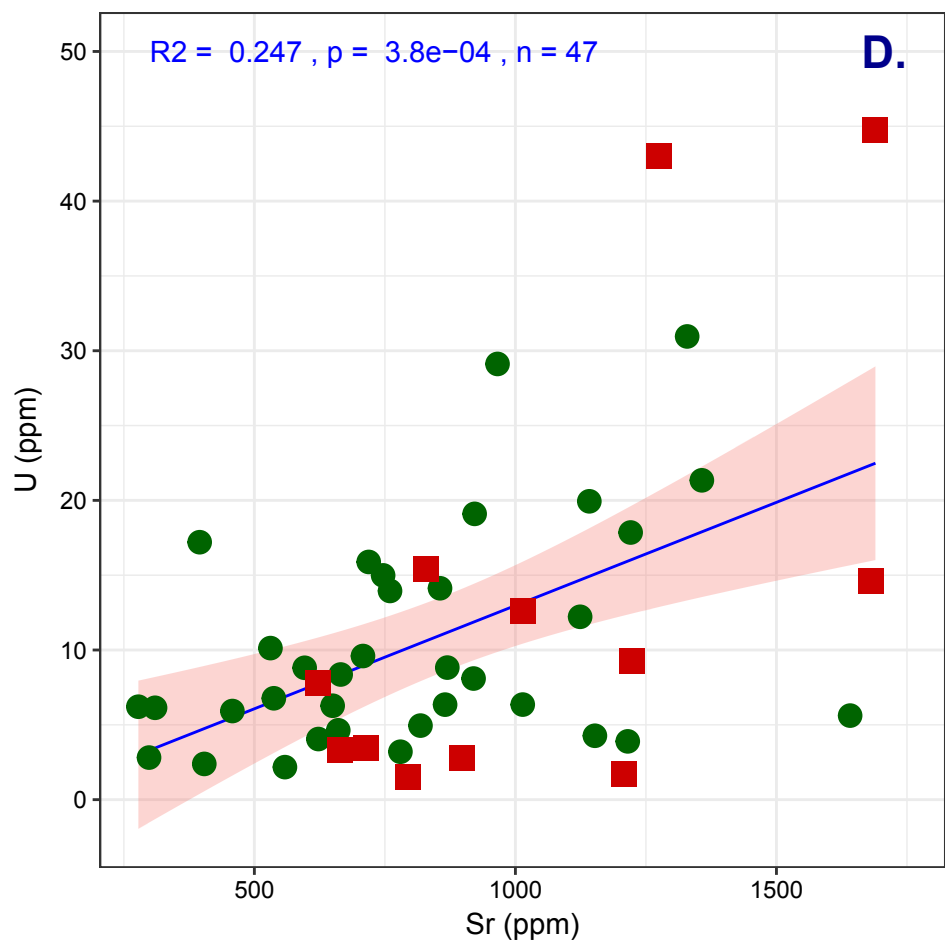
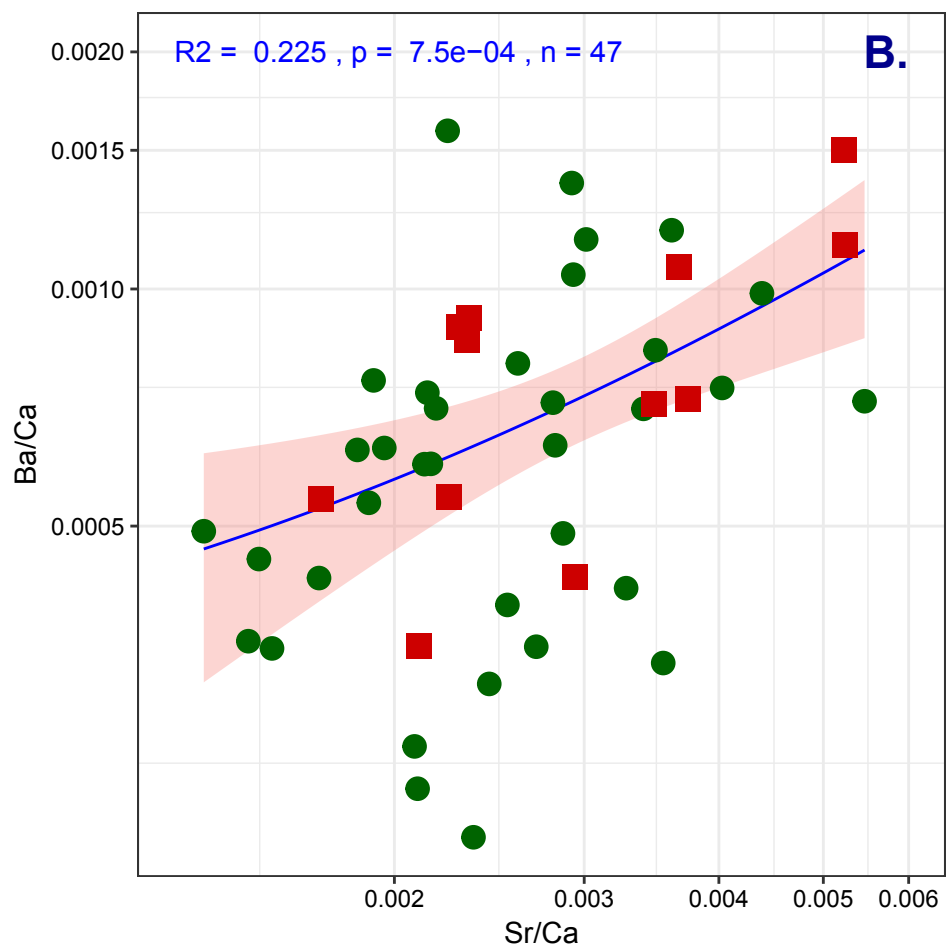
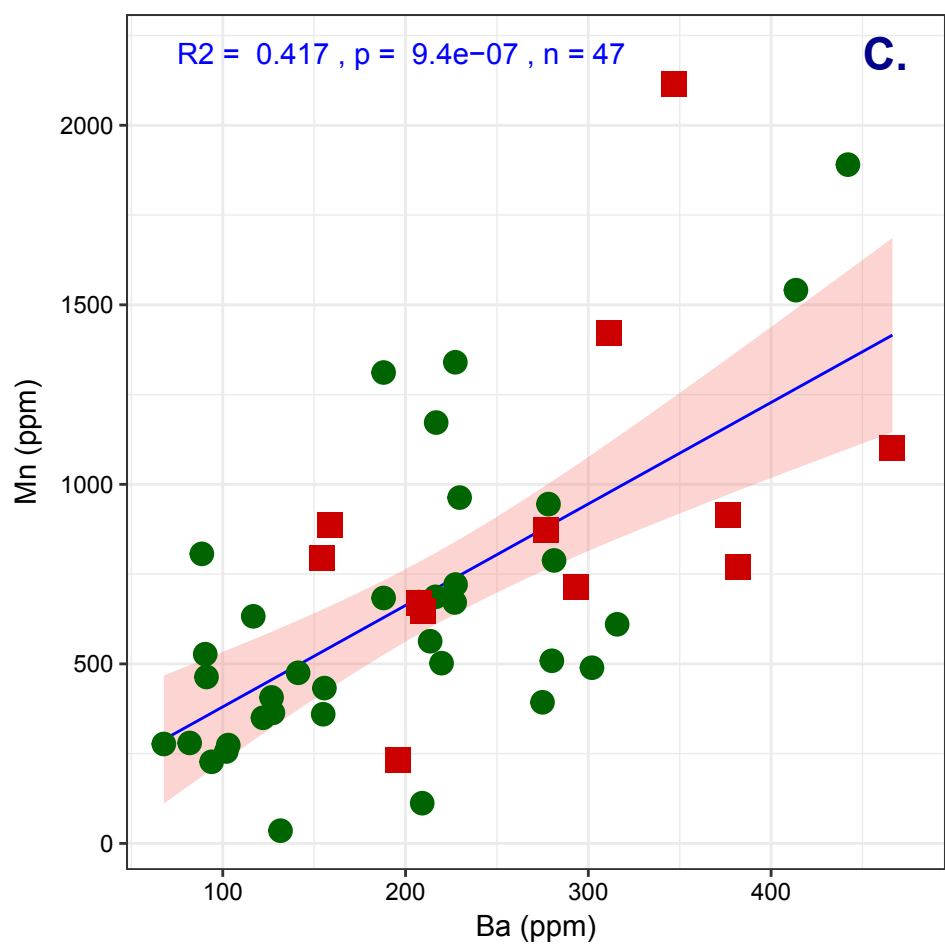
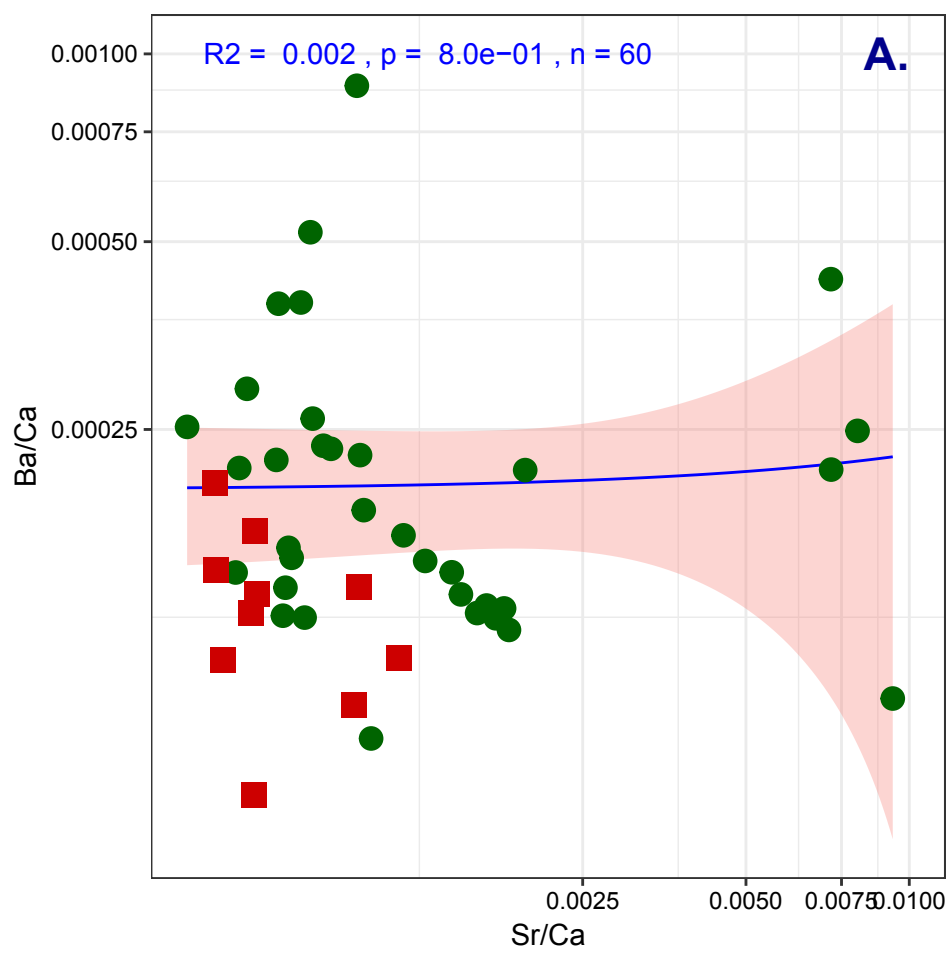
#### References

- 1 Amini et al. 2008 Geoch. Cosm. Acta. 72(16), 4107-4122.
- 2 Amini et al. 2009 Geostand. Geoanal. Res. 33(2), 231-247.
- 3 Böhm et al. 2006 Geoch. Cosm. Acta. 70(17), 4452-4462.
- 4 Chang et al. 2004 Biochem. Biophys. Res. Comm. 323(1), 79-85.
- 5 Cobert et al. 2011 Rapid Comm. Mass Spec. 5(19), 2760-2768.
- 6 Colla et al. 2013 Geoch. Cosm. Acta. 121, 363-373.
- 7 Fantle 2015 Geoch. Cosm. Acta. 148, 378-401.
- 8 Farkas et al. 2007 Earth. Planet. Sci. Lett. 253(1-2), 96-111.
- 9 Farkas et al. 2007 Geoch. Cosm. Acta. 71(21), 5117-5134.
- 10 Farkas et al. 2011 Geoch. Cosm. Acta. 75(22), 7031-7046.
- 11 Feng et al. 2016 Geostand. Geoanal. Res. 41(1)
- 12 Gussone et al. 2003 Geoch. Cosm. Acta. 67(7), 1375-1382.
- 13 Harouaka et al. 2014 Geoch. Cosm. Acta. 184, 114-131.
- 14 Hassler et al. 2018 Proc. Roy. Soc. B 285(1876), 20180197.
- 15 Heuser and Eisenhauer 2008 Geostand. Geoanal. Res. 32(3)
- 16 Heuser et al. 2002 Int. J. Mass. Spec. 220(3), 385-397.
- 17 Heuser et al. 2005 Paleoceno. Paleoclim. 20(2).
- 18 Heuser et al. 2011 Geoch. Cosm. Acta. 75(12), 3419-3433.
- 19 Heuser et al. 2016 Isotopes. Environ. Health Stud. 52(6), 633-648.
- 20 Hindshaw et al. 2011 Geoch. Cosm. Acta. 75(1), 106-118.
- 21 Hindshaw et al. 2013 Earth. Planet. Sci. Lett. 374, 173-184.
- 22 Hippler et al. 2003 Geostand. Newslett. 27(1), 13-19.
- 23 Holmden et al. 2010 Geoch. Cosm. Acta. 74(3), 995-1015.
- 24 Holmden et al. 2012 Geoch. Cosm. Acta. 83, 179-194.
- 25 Huang et al. 2010 Earth. Planet. Sci. Lett. 292(3-4), 337-344.
- 26 Huang et al. 2012 Geoch. Cosm. Acta. 77, 252-265.
- 27 Jacobson and Holmden 2008 Earth. Planet. Sci. Lett.
- 28 Jacobson et al. 2015 Earth. Planet. Sci. Lett. 416, 132-142.
- 29 Kasemann et al. 2008 Earth. Planet. Sci. Lett. 270(3-4), 349-353.
- 30 Lehn and Jacobson 2015 J. Anal. At. Spec. 30(7), 1571-1581.
- 31 Li et al. 2015 Chem. Geol. 422, 1-12.
- 32 Martin et al. 2015 Chem. Geol. 415, 118-125.
- 33 Martin et al. 2017a Curr. Biol. 27, 1641-1644.
- 34 Martin et al. 2017b Palaeontology 60, 485-502.
- 35 Melin et al. 2014 American J. Phys. Anthr. 154(4), 633-643.
- 36 Mueller et al. 2011 Geoch. Cosm. Acta. 75(8), 2088-2102.
- 37 Nielsen et al. 2012 Handbook Environ. Isotope. Geochem. 105-124
- 38 Nielsen and DePaolo 2013 Geoch. Cosm. Acta. 118, 276-294.
- 39 Ockert et al. 2013 Geoch. Cosm. Acta. 112, 374-388.
- 40 Reynard et al. 2011 Geoch. Cosm. Acta. 75(13), 3726-3740.
- 41 Romaniello et al. 2015 J. Anal. At. Spec. 30(9), 1906-1912.
- 42 Schiller et al. 2012 J. Anal. At. Spec. 27(1), 38-49.
- 43 Schmitt et al. 2003 Geoch. Cosm. Acta. 67(14), 2607-2614.
- 44 Schmitt et al. 2009 J. Anal. At. Spec. 24(8), 1089-1097.
- 45 Schmitt et al. 2013 Geoch. Cosm. Acta. 110, 70-83.
- 46 Simon and DePaolo 2010 Earth. Planet. Sci. Lett. 289(3-4), 457-466.
- 47 Skulan and DePaolo 1999 Proc. Nat. Acad. Sci. 96(24), 13709-13713.
- 48 Skulan et al. 1997 Geoch. Cosm. Acta. 61(12), 2505-2510.
- 49 Skulan et al. 2007 Clin. Chem. 53(6), 1155-1158.
- 50 Steuber and Buhl 2006 Geoch. Cosm. Acta. 70(22), 5507-5521.
- 51 Tacail et al. 2014 J. Anal. At. Spec. 29(3), 529-535.
- 52 Tacail et al. 2016 J. Anal. At. Spec. 31(1), 152-162.
- 53 Tacail et al. 2017 Proc. Nat. Acad. Sci. 201704412.
- 54 Teichert et al. 2009 Earth. Planet. Sci. Lett. 279(3), 373-382.
- 55 Tipper et al. 2010 Global Biogeochem. Cycles 24(3).
- 56 Used for conversion
- 57 Wieser et al. 2004 J. Anal. At. Spec. 19(7), 844-851.
- 58 Wombacher et al. 2009 J. Anal. At. Spec. 24(5), 627-636.
- 59 Zhu et al. 2015 Geostand. Geoanal. Res. 40(2).

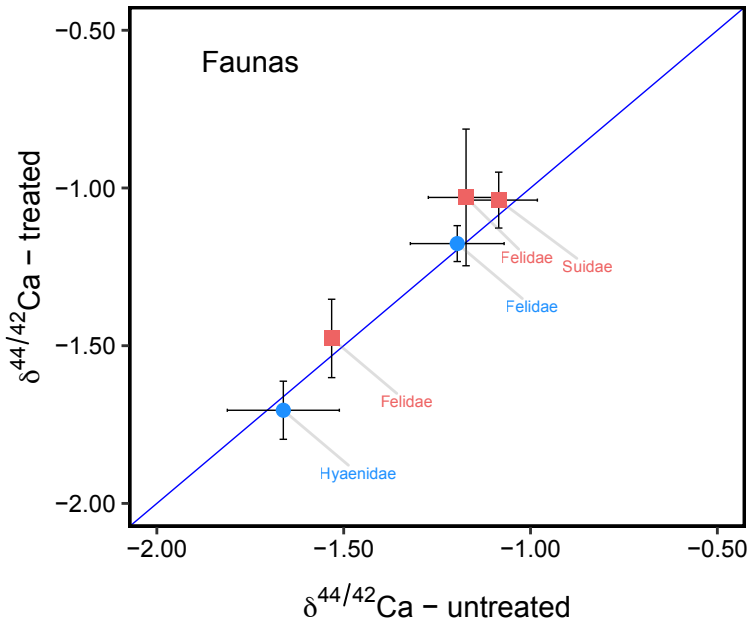












■ Fossil    ● Modern